Escola de Camins
Escola Tècnica Superior d'Enginyeria de Camins, Canals i Ports
UPC BARCELONATECH

BACHELOR FINAL THESIS

Sedimentary evidences of paleotsunamis in the Mediterranean Sea: accumulation of large boulders along the coastline and mass transport deposits.

Final Thesis developed by:

Bernat Perelló, Josep

Directed by:

Canals Artigas, Miquel

Gelabert Ferrer, Bernadí

Bachelor in:

Geological Engineering

Barcelona, 15/06/2018

Department of Earth and Ocean Dynamics

Acknowledgements

I would like to express my sincerest gratitude to my advisor, Professor Canals, who provided me the fantastic opportunity to work in this scientific branch. Moreover, I would like to thank him for providing all the research facilities and for reviewing my project.

I also wish to thank Professor Bernadí Gelabert, who helped me with the recognition of the Mallorca zones and also with the data.

Furthermore, I wish to thank Nieves Lantada. His help with GIS project was also very appreciated because he solved all my doubts that I had during all the procedure.

Finally, I wish to express my deepest gratitude to my family for their emotional and economical support.

Abstract

Several studies have shown the presence, throughout the coasts and basins of the Mediterranean Sea, of numerous deposits created by tsunamis. Coastal deposits consist mainly of large blocks, often imbricated, at variable levels above the current sea level. In the deep margins and basins mass tsunami deposits are made of mass transfer deposits (MTDs), dominated by turbidites and homogenites. Some of these deposits have been correlated with historical tsunamis.

Knowledge on tsunami deposits is essential to perform hazard studies and risk maps. This thesis summarizes the result of an extensive bibliographic research and fieldwork about sedimentary evidences of paleo-tsunamis in the Mediterranean Basin.

The production of a synthesis map with the help of a GIS software has been a key task. Such as a map could be useful for tsunami hazard assessment and impacts in Mediterranean shore-lines.

Resum

Diversos estudis han demostrat la presència de nombrosos dipòsits generats per tsunamis a les costes i conques pregones de la mar Mediterrània. Els depòsits costaners consisteixen principalment en grans blocs, sovint imbricats, situats a cotes variables per sobre del nivell actual del mar. Als marges i conques pregones hi ha dipòsits de transport de massa, dominats per turbidites i homogenites. Alguns d'aquests dipòsits s'han correlacionat amb tsunamis històrics.

El coneixement dels dipòsits és essencial per realitzar estudis i mapes de riscos. Aquest treball resumeix el resultat d'una recerca bibliogràfica extensiva i de treball de camp sobre les evidències sedimentàries de paleo-tsunamis a la conca Mediterrània, amb l'accent en la seva regió occidental.

La confecció d'un mapa amb l'ajuda d'un programari SIG ha estat una tasca clau d'aquest treball. Aital mapa podria ser útil per l'avaluació del risc de tsunamis i llurs impactes a les costes de la Mediterrània.

Table of contents

Figures list

Tables list

1. Introduction

The Mediterranean Basin was formed as a consequence of the ancient African-Arabian plate colliding with the Eurasian plate. The broad line of collision pushed up a very long system of mountains from the Pyrenees in Spain to the Zagros Mountains in Iran in an episode of mountain-building tectonics known as the Alpine orogeny. Accordingly, the Mediterranean Basin consists of several stretched and subducting tectonic microplates.

1.1 Geological setting

Because of its location at the boundary of two main tectonic plates, to the Mediterranean Basin hosts a high seismicity level which is, in its western domain, essentially expressed in a moderate, diffused seismic area, in northern Africa as shown in figures 1 and 2. Northern Algeria is part of the collision zone, where geodetic studies indicate an actual plate convergence rate of about 5.0±1mm/year in a N60 W direction (Calais et al., 2003; Nocquet and Calais, 2003, 2004; Serpelloni et al., 2007). Earthquakes with magnitude Mw>5 frequently occur in the area (Harbi et al., 1999; Aoudia et al., 2000; PeláezMontilla et al., 2003), sometimes inducing significant destruction and casualties (Adams and Barazangi, 1984). Well-studied thrusting earthquakes essentially occur onshore, as for instance the largest recorded Ms 7.3 1980 El Asnam earthquake (Ruegg et al., 1982; Deschamps et al., 1982; Meghraoui et al., 1988; Bezzehgoud et al., 1995). According to available catalogues, tsunamis are frequent in Mediterranean and associated with both earthquakes and underwater landslides occurring on margins with steep slopes (Maramai et al., 2003; Papadopoulos and Fokaefs, 2005).

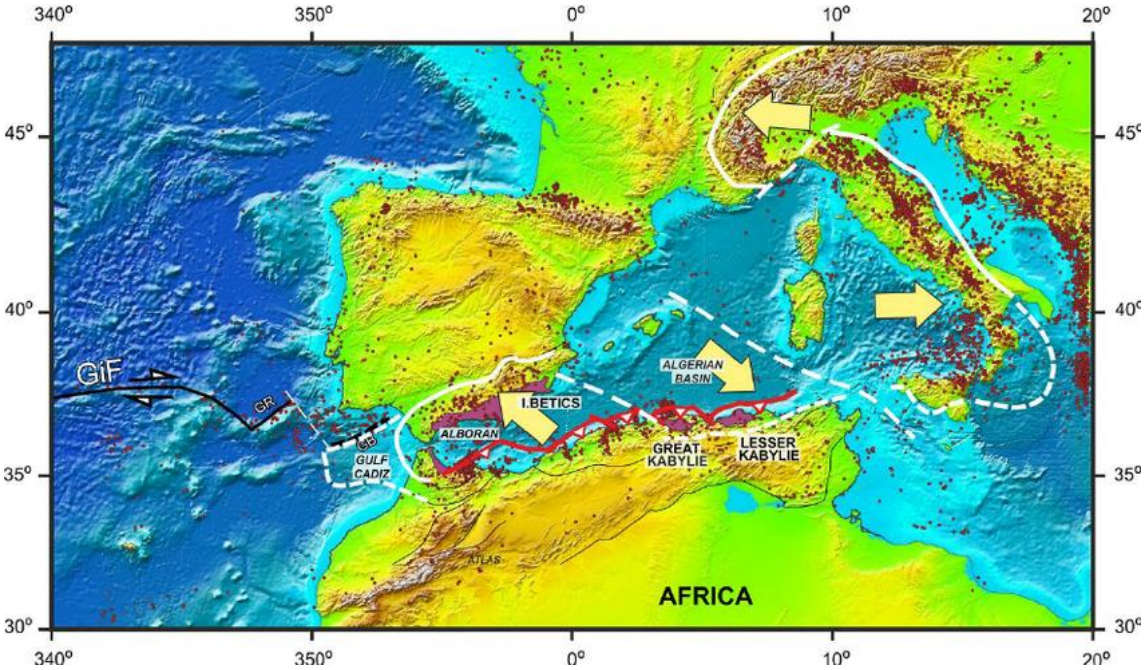

Figure 1: The main Algerian fault (Casciello et al., 2015).

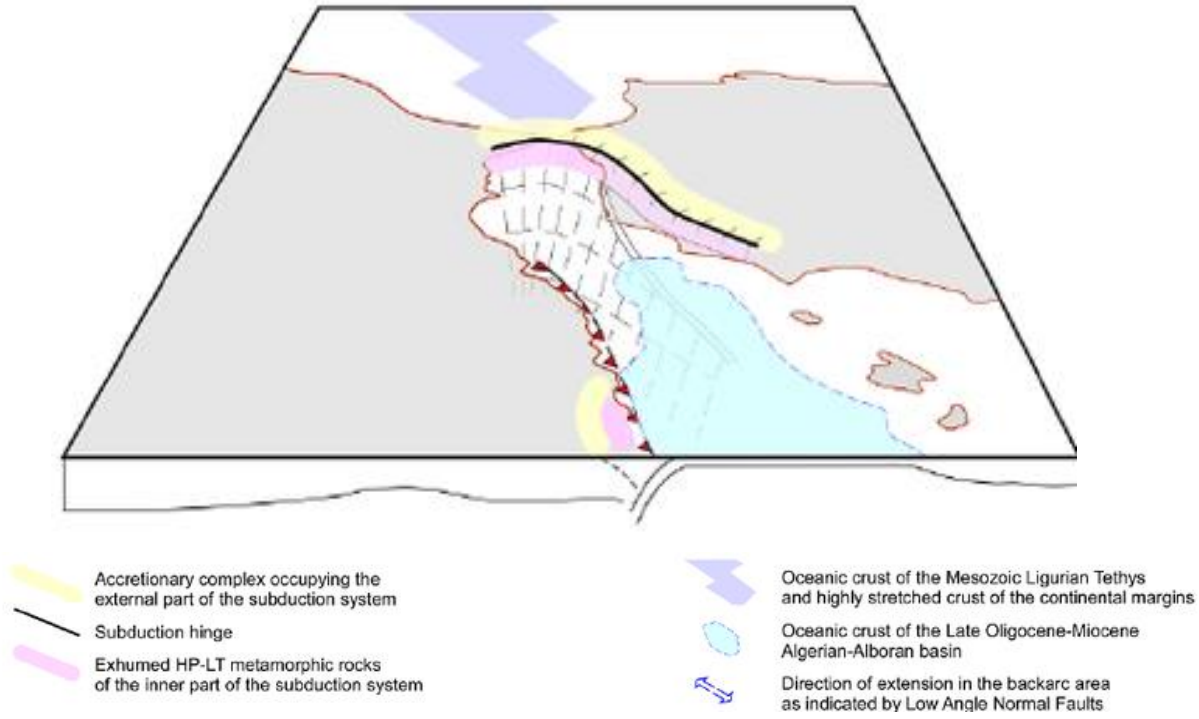

Figure 2: The same fault as in figure 1 viewed from another perspective (Casciello et al., 2015).

Although the North Algerian margin is not positioned above a subduction zone, many earthquakes and landslides along it are recorded each year and some destructive tsunamis have been reported over the past 700 years, three resulting from great earthquakes in 1365, 1856 and 2003 (Yelles, 1991; Mokrane et al., 1994; Soloviev et al., 2000; Tinti et al., 2001; Alasset et al., 2006).

Recent studies along the Algerian margin have greatly improved knowledge on active structures. They brought to light the presence of compressional deformation features during the Quaternary period with inverse faults (pure compressive deformation) and strike slip faults leading to a clear seismogenic zone along the margin (Domzig, 2006). The tsunamis generated during contemporary offshore earthquakes could have huge consequences on the Algerian coast, which is considered as “near field” (less than 100 km) (Yelles et al., 2004). But it could also have consequences in the Balearic Islands especially in harbors or bays where side effects are rather common, including wave arrivals up to 1m high in 2003, when the last significant tsunamigenic earthquake took place in Algeria (Vela et al., 2014). It is also worth mentioning that some harbors in the Balearic Islands located all along the southern coastline of Menorca and Mallorca, as well as Mahon, Ciutadella or Palma, were damaged in 2003. Harbors and embayments in the Baleares can exhibit special behavior to tsunami arrival, directly due to their natural oscillation mode or to the resonant oscillation of the water body, inducing the so-called *seiches* (Monserrat et al., 1991; Gomis et al., 1993; Rabinovich and Monserrat, 1996 and 1998; Liu et al., 2003; Jansa et al., 2007). The 2003 event also affected Côte

d'Azur , where several witness accounts report oscillations and eddies in several harbors consecutive to the earthquake and associated tsunami (A. Sahal, pers. comm., 2007).

1.2 Tsunami hazards

In the last two decades the interest of the scientific community in tsunami studies has increased significantly, especially in terms of hazard assessment and risk reduction. The occurrence of the catastrophic Indonesian (2004) and Tohoku (2011) tsunamis lighted out the necessity of taking adequate countermeasures to protect coastal areas from this threat and implement tsunami warning systems in all the regions prone to them. In this context, the attention of scientists was also drawn on the European area where the tsunamigenic hazard was for long time underestimated. The European Union (EU) answered this demand by financing scientific projects on tsunami research in the Euro-Mediterranean area in order to develop strategies for tsunami risk reduction (Maramai et al., 2003).

One of the last EU financed project was TRANSFER (Tsunami Risk ANd Strategies For the European Region, 2006-2009), which aimed at improving the knowledge on tsunami processes in the Euro-Mediterranean area, in particular assessing the risk associated with tsunami and establishing risk methodologies and risk reduction policies, from prevention to mitigation. The project maintained the continuity with previous European projects such as GITEC and GITEC-TWO. One of the main goals of the project was the upgrading of the GITEC-TWO tsunami catalogue that covers the same area and was the result of efforts of various European research groups co-operating in these EU projects.

Another EU project was ASTARTE (Assessment, Strategy And Risk Reduction for Tsunamis in Europe, 2007-2013), which among many other goals aimed at compiling and critically analyzing former results on the identification of mass transport deposits (MTDs) and other types of deposits that could have been caused by tsunamis within the North-Eastern Atlantic, Mediterranean and Connected Seas Region (NEAM Region).

State of the art

2.1 Introduction to tsunamis

Tsunamis are single or sets of long shallow water waves, usually observed in oceans or in large lakes. They are associated with a sudden displacement of the water column due to a numberof various trigger mechanisms including earthquakes, submarine or subaerial gravitative masswastings, volcanism, cosmic impacts or atmospheric disturbances. Mistakenly called oshio at first (from Japanese high tide), later the term tsunami was introduced for this wave phenomenon (Parker 2010, p. 140; Goff et al. 2016), meaning harbour (tsu) wave (nami). This term relates to the fact that tsunamis, due to their long wavelengths, are often not perceived in the open sea but form their destructive power near the coast, especially in marine inlets or in harbours, where the waves undergo significant shoaling and funnelling.

With coasts becoming increasingly popular as places of residence, tourism and industry (Mc-Granahan et al. 2007, pp. 18–21), tsunamis are a major threat to today's society. Recent events in south-east Asia (2004) and Japan (2011) have demonstrated the tremendous power of tsunamis on coastal landscapes resulting in huge human and economic losses. According to the global historical tsunami database (NDGC/WDS 2015a), altogether about 940.000 deaths have been counted in connection with tsunami impacts worldwide during prehistorical, historical and modern times. Adding an unknown number of unrecorded victims especially associated with pre-historical tsunami events, the actual death toll must be assumed to be well above one million people. The total amount of economic loss is even more difficult to estimate. Solely regarding the two most destructive events in recent history, estimates of the total financial damage range from $ 15 billion to $ 80 billion for the Indian Ocean tsunami in 2004 (Bryant 2008, p. 177) and up to $ 335 billion with respect to the To¯hoku tsunami and earthquake in Japan (2011) for the year 2011 alone (Daniell & Vervaeck 2012, p. 17). The latter event was the costliest natural disaster ever recorded.

Stimulated by recent tsunami events, geoscientific research of this natural phenomenon has significantly increased during the last decades, in particular since the Indian Ocean tsunami in 2004 (e.g. Keating 2006, pp. 392, 393; Santiago-Fandiño et al. 2018). The main topics of tsunami science are numerical and experimental modelling of tsunami generation, propagation and inundation (including effects of vegetation, buildings etc.), field surveys in search of on- and offshore sedimentary and geomorphological traces of pre-historical tsunami impacts, research on tsunamigenic earthquakes and gravitational mass wastings as well as the observation of tsunami waves in the oceans and along coasts using, e.g. DART (Deep-ocean Assessment and Reporting of Tsunamis)-buoys, satellites or other instruments (Keating 2006, pp. 388, 389). Recent years have seen major advances in these research fields, which have considerably improved the understanding of the tsunami waves. Accordingly, also tsunami forecast techniques have extended and significantly gained in reliability. An outstanding example for this is the German-Indonesian Tsunami Early Warning System (GITEWS), initiated after the

2004 Indian Ocean Tsunami, which consists of several seismometers as well as GPS and gauge stations (e.g. Rudloff et al. 2009 and further articles in the same special issue). Although a reliable tsunami hazard assessment still does not prevent the impact itself, the progress in tsunami science and forecast techniques as well as the increasing awareness of this coastal hazard during the last decades and particularly since 2004 has certainly reduced the potential number of tsunami victims in recent history worlwide (Rabinovich et al. 2015, pp. 615, 616).

2.2 Source mechanisms

A tsunami can be generated by any abrupt disturbance of the sea-surface. There are different mechanisms capable of generate a tsunami. The most frequent source mechanisms are earthquakes. Events like landslides volcanic eruptions, and/or object impacts on the water surface (e.g. meteoritic impacts) are other source mechanisms capable of generating tsunamis.

- Earthquakes:

The most common sources in the tsunami generation are earthquakes produced in marine and coastal regions by the vertical movement of active faults (Figure 3). The fault movement mechanism is based on the Plate Tectonics, that describes an earth model characterized by a small number of lithospheric plates, that float on a viscous under layer called the asthenosphere. These plates, which cover the entire surface of the earth and contain both the continents and seafloor, move relative to each other at different rates. The region where two plates come in contact is called a plate boundary, and the way in which one plate moves relative to another determines the type of boundary:

I. Spreading: Where the two plates move away from each other (e.g. Middle Atlantic spreading ridge).
II. Transform: Where the two plates slide horizontally past each other without destruction or generation of crust (e.g. San Andreas or Alpine faults).
III. Subduction: Where the two plates move toward each other, and one slides beneath the other (e.g. Nankai or Sumatra subduction zones). Subduction is the principal cause for major tsunamis.

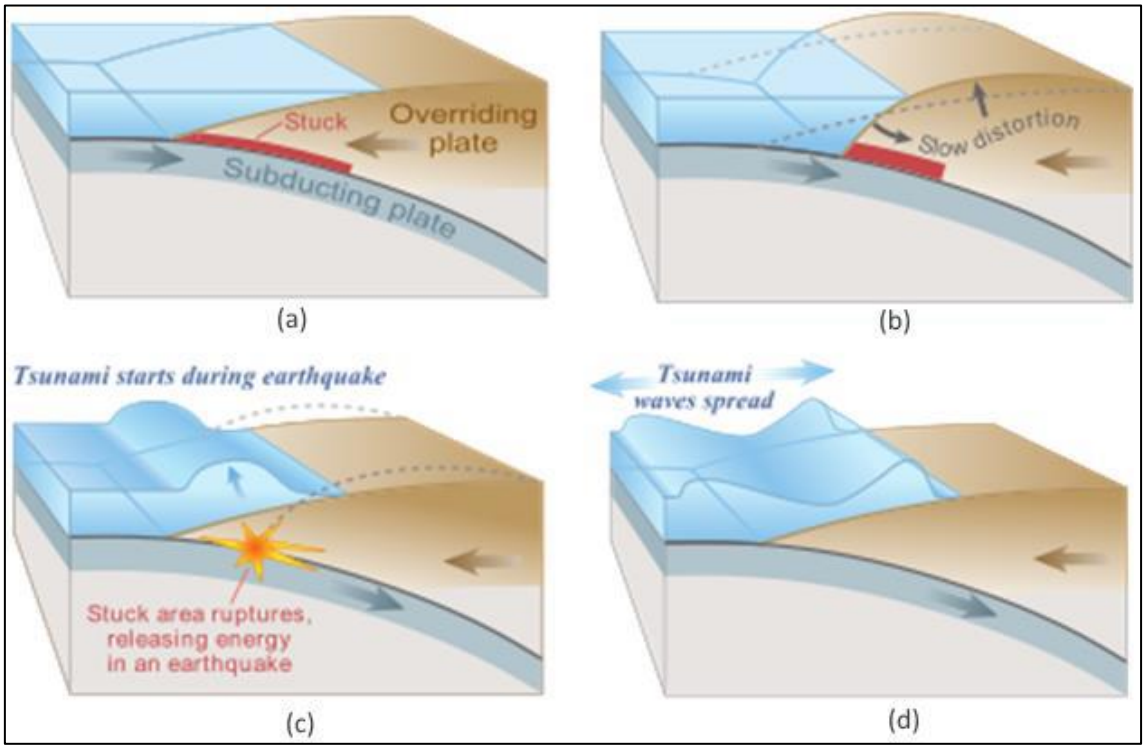

Figure 3: Generation process for a tsunami triggered by an earthquake in a subduction zone: (a) when two different plates come in contact, the sides of the fault move past each other. Due to the irregularities and asperities in the fault surface the fault gets locked and the frictional resistance increases; (b) the relative motion between plates continues, increasing the stress and therefore storing strain energy in the fault surrounding area; (c) hen the stress accumulated is sufficient to break the irregularities blocking the fault, the plates slide releasing the stored energy in a short time period, the earthquake, and (d) this energy is transferred to the sea floor and moves it vertically, generating an abrupt sea-surface disturbance (Atwater et al., 2005).

Not all earthquakes generate tsunamis. To generate a tsunami, the fault movement responsible for the earthquake must be underneath or near the seafloor and cause its vertical movement (up to tens of meters) over a large area (from hundred to thousand square kilometres). Other factors involved in the tsunami generation mechanism are the simultaneous occurrence of underwater landslides due to the shaking, and the efficiency with which energy is transferred from the earth's crust to the ocean water.

Different parameters are necessary to characterize the dislocation or slip motion that will deform the surface producing the seafloor displacement because of the earthquake (Figure 4 and Table 1). These parameters describe the fault plane, where the motions between faults take place, and its associated movement, and are:

Parameters	Units
Epicenter (Lat, Lon)	Degrees
Focal depth	Meters
Length of Fault Plate	Meters
Width of Fault Plane	Meters
Strike direction θ	Degrees
Dip angle δ	Degrees
Slip length	Meters
Slip Angle λ	Degrees

Table 1: Parameters for the Elastic Fault Plane Model (Sorensen et al., 2006).

- Epicenter: The projection of the earthquake focus on the Earth surface. This parameter is indicated by geographic coordinates (latitude and longitude).
- Focal depth (h): Vertical distance between the earthquake focus and the epicenter.
- Length (L): Distance measured along the top edge or bottom edge and parallel to the strike direction.
- Width (W): Distance measured between the top and the bottom edges and perpendicular to the strike direction.
- Strike direction (θ): Angle formed the fault plane in relation to the geographic north and measured clockwise
- Dip angle (δ): Angle formed between the Earth surface and the fault plane. It is measured from the Earth surface down to the fault plane.
- Slip length: Motion distance of the sliding block relative to the foot block along the strike direction on the fault plane.
- Slip angle (λ): Slide direction relative to the foot block on the fault plane.

At present the location and magnitude of an earthquake is measurable nearly immediately thanks to the advent of modern seismometers, digital recording, and real-time communication links. This allows warning centres to provide initial tsunami warnings within minutes after the earthquake's occurrence.

The moment magnitude (Mw, with the subscript "w" meaning mechanical work performed) is a dimensionless number defined by Hanks and Kanamori (1979) as:

$$MW = \frac{2}{3}\log(M(0)) - 10.7Mw \quad (1)$$

Where M_0 is the seismic moment in Nm. The constant values in the equation are chosen to achieve consistency with the magnitude values produced by earlier scales, the Local Magnitude and the Surface Wave magnitude, both referred to as the "Richter" scale by reporters. Moment magnitude is now the most common measure for medium to large earthquakes, but breaks down for smaller quakes. For example, the USGS does not use this scale for earthquakes with a magnitude of less than 3.5, which is the great majority of quakes.

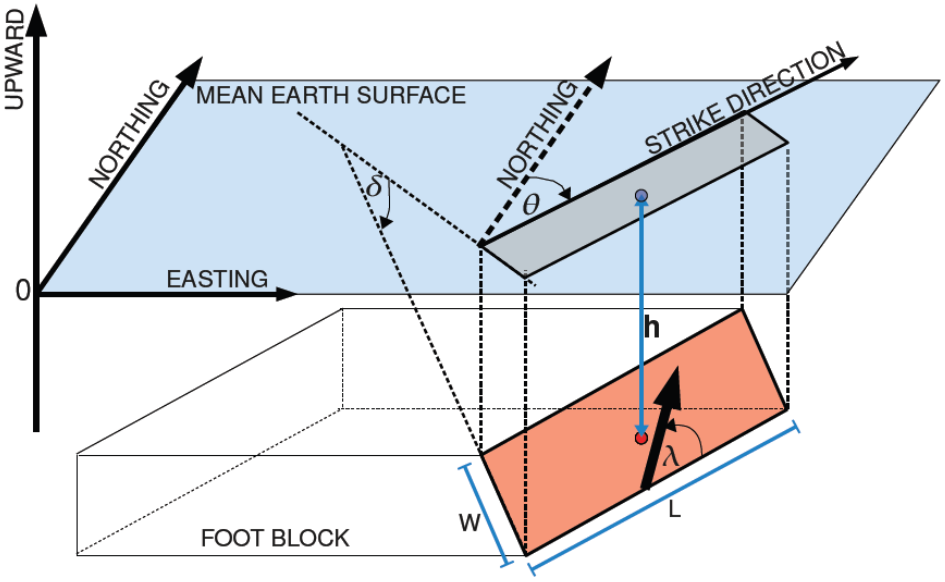

LEGEND

	MEAN EARTH SURFACE
	FAULT PLANE (A RECTANGULAR SURFACE ON FOOT BLOCK)
	PROJECTION OF FAULT PLANE ON MEAN EARTH SURFACE
	SLIP DIRECTION ON FAULT PLANE (RELATIVE TO FOOT BLOCK)
	FOCUS OF AN EARTHQUAKE (CENTER OF FAULT PLANE)
	EPICENTER (PROJECTION OF FOCUS ON EARTH SURFACE)
δ	DIP ANGLE OF FAULT PLANE
λ	SLIP DIRECTION ON FAULT PLANE (RAKE ANGLE)
θ	STRIKE ANGLE
h	FOCAL DEPTH
L	LENGTH OF FAULT PLANE
W	WIDTH OF FAULT PLANE

Figure 4: Sketch of a fault plane and fault parameter definitions (COMCOT User Manual v.17, 2009).

Shallow focus earthquakes along subduction zones are responsible for most destructive tsunamis. The Lisbon earthquake (1755), the Great Chilean Earthquake (1960), Indian Ocean earthquake (2004) and Tohoku earthquake (2011) are examples of large earthquakes that have generated catastrophic tsunamis.

- Landslides

Landslides are produced when ground or other material slide down a slope. Different factors have influence in the generation of a common landslide:

I. Slope angle
II. Climate
III. Weathering
IV. Water content
V. Vegetation
VI. Overloading
VII. Geology

It can be different elements contributing to a landslide but usually one triggers the material movement. Landslides can take place in the surface or undersea, which often occur during large earthquakes. Both superficial and submarine landslides can generate localised tsunamis.

Superficial landslides disturb the water from above the water surface. The falling debris disturbs the water equilibrium position and produce a tsunami. Tsunamis generated by non-seismic mechanisms usually dissipate swiftly and is unusual they affect coastlines far from the generation point.

Undersea landslides take place when a large amount of sediment is displaced on the seafloor. During a submarine landslide the sediment movement along the sea-floor modify the equilibrium in the water surface. The perturbation of the sea-level generates a tsunami that will be propagated by gravitational forces.

Underwater landslides triggered by earthquakes can generate destructive tsunamis. On July 17th, 1998 a tsunami devastated the north-western coast of Papua New Guinea. Apparently, an earthquake triggered a large underwater landslide. Consequently, three waves measuring more than 7-meter-high struck a 10km stretch of coastline within ten minutes of the earthquake.

- Volcanic eruptions

Violent marine volcanic eruptions can create, similarly to landslides, an impulsive force that displaces the water column and generates a tsunami. Tectonic movements can also cause tsunamis resulting from volcanic activity, caldera collapses or flank failures into a water body or by pyroclastic flow discharge into the sea (Figure 5).

On August 27th, 1883 Krakatoa erupted causing the largest and more catastrophic volcanic tsunami in history. The tsunami was formed just under a minute after the explosion, and it grew up to a 40 meters wave height. It is estimated this tsunami caused over thirty-six thousand casualties. There was a second explosion, generated when the

magma chamber collapsed and allowing the seawater rush into the magma chamber creating a second tsunami, smaller than the first one.

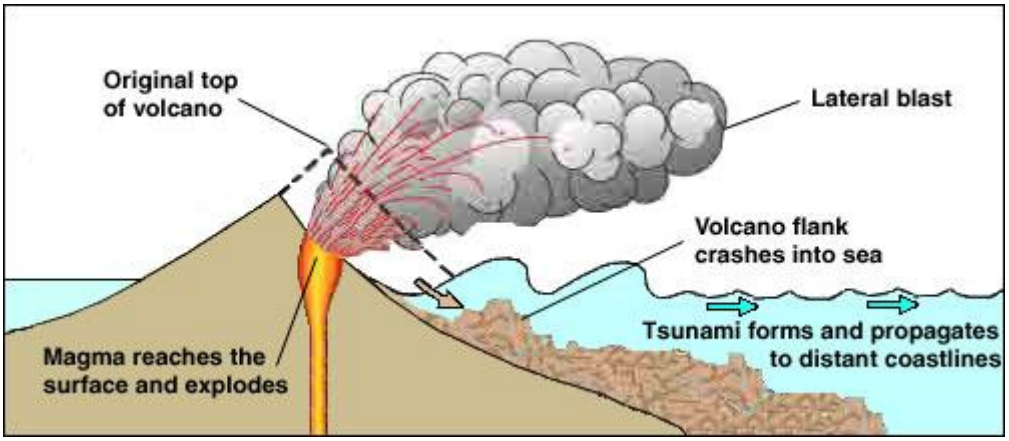

Figure 5: The debris avalanche crashes into the sea once it travels down the volcanoes side pushing the water up as they meet (Khoury, 2012).

- Object impacts

Any disturbance of the water surface can generate a tsunami. Superficial landslides and volcanic eruptions can disturb the sea surface with object impacts from above the water level. Space borne objects such meteorites, asteroids and comets also can disturb the sea surface generating a tsunami, but the probabilities of a space object impact are very small.

Gersonde et al. (1997) found evidence of a 4km diameter asteroid that landed offshore of Chile approximately 2 million years ago. Their studies conclude that its collision may have produced a huge tsunami capable to swept portions of South America and Antarctica.

Since scientists cannot predict when earthquakes or other tsunami sources will occur, neither their dimensions, they cannot determine exactly when a tsunami will be generated and its size. However, by looking at past historical tsunamis, scientists know where tsunamis are most likely to be generated. Past tsunami height measurements are useful in predicting future tsunami impact and flooding limits at specific coastal locations and communities. Paleotsunami research, in which scientists look for sediments deposited by giant tsunamis, is helping to extend the documented historical tsunami record further back in time.

2.3 Wave propagation

The process to model the wave propagation using all the elements involved is extremely complex. A three-dimensional analysis with the interaction between wind, the bottom surface, obstacles and currents, will require very complex equations and too many calculations. However, the small amplitude wave theory simplifies the mathematics

involved considerably. A great number of observations can be explained studying two-dimensional, monochromatic and progressive waves. Tsunamis wavelengths vary from tens to hundreds of kilometres and travel in the deep ocean with only a few centimetres height. Therefore, the small amplitude assumptions can be applied for tsunamis when they are located offshore.

The main physical characteristics that define a wave (Figure 6) are the wave height (H), the wave amplitude (a), the wavelength (L) and the water depth (D).

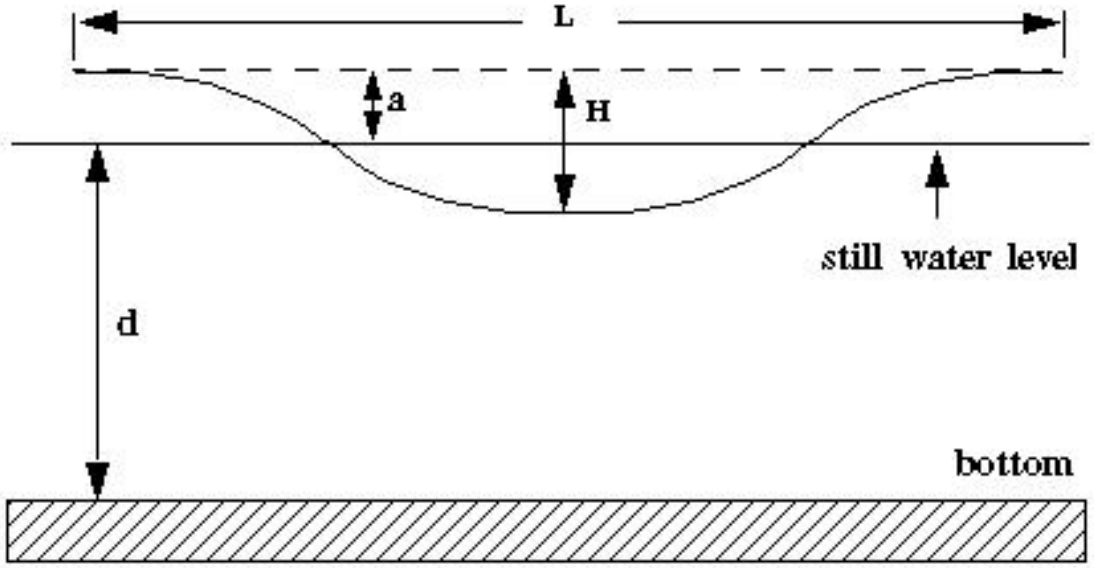

Figure 6: Wave characteristics. H: wave height; a: wave amplitude; L: wave length; and D: water depth (Sorensen et al., 2006).

Other parameters are the wave period and the celerity. The wave period (T) is the time between consecutive crests in a fixed point. Celerity (C) is the wave speed, the distance travelled by a wave crest, the wave length, per unit time. The relation between celerity, period a length is:

$$C = \frac{L}{T} \tag{2}$$

The small amplitude theory assumes that a/L and a/d are small. Making use of this assumption the wave celerity is function of both the wave length (L) and the water's relative depth (d/L). Solving the equation of motion for small amplitude waves yields the following equation for the wave celerity.

$$C = \sqrt{\frac{gL}{2\pi} \cdot \tan(\mathrm{h}) \left(2\pi \frac{D}{L}\right)} \tag{3}$$

Where **g** is the gravitational acceleration.

The hyperbolic tangent function has limit forms for both small and large values of its argument, so it is useful to classify waves according to the relative depth (Table 2).

Relative Depth	Wave pattern	Wave celerity	Wave length
$\frac{D}{L}$ < 0.05	Shallow water wave	$\sqrt{g \cdot D}$	$\sqrt{T \cdot g \cdot D}$
0.05 < $\frac{D}{L}$ < 0.5	Intermediate depth water	$C = \sqrt{\frac{gL}{2\pi} \cdot \tan(\mathrm{h})\left(2\pi \frac{D}{L}\right)}$	$\frac{g \cdot T^2}{2\pi} \cdot tan\, h \cdot \left(2\pi \cdot \frac{D}{L}\right)$
$\frac{D}{L}$ > 0.5	Deep water wave	$\sqrt{\frac{q \cdot L}{2\pi}}$	$\frac{g \cdot T^2}{2\pi}$

Table 2: Relation between the relative depth, the wave patterns and the wave's characteristics (Sorensen et al., 2006).

In deep ocean waters tsunamis have periods typically from 10 minutes to one hour and wave lengths of several hundreds of kilometres. When a 200km wave length tsunami passes over a 4km depth, the average depth of the oceans, the relative depth is D/L=0.02. Since this relative depth is less than 0.05, this tsunami is a shallow-water wave. For shallow waves the celerity depends only on the water depth. Knowing the bathymetry, the wave celerity and its propagation can be estimated. Figure 7 shows the relation between water depth, velocity and wavelength in tsunamis.

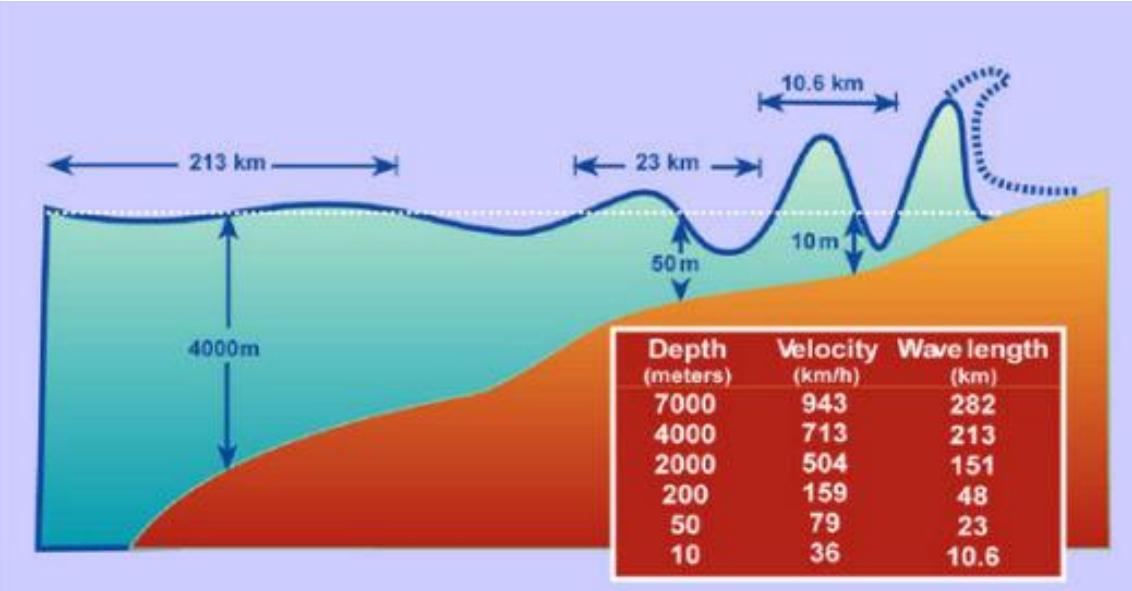

Figure 7: Wave propagation (NEA, http://www.nea.gov.sg/training-knowledge/weather-climate/tsunami).

Shallow waves are affected by shoaling, refraction and diffraction. Because of their characteristics, tsunamis are affected by these processes even in the deep ocean.

- Shoaling

When the waves enter in shallower waters the wave celerity slows. Because the wave period remains the same the wave length decreases. Thus, the tsunami's energy flux remains nearly constant. Given that the energy flux depends on group celerity and wave height, as the tsunamis travel into shallower waters its wave height (H) grows. An unnoticeable tsunami at sea may grow several meters in height near the coast because of the shoaling.

Shoaling relates the tsunami's wave height with the depths by the equation:

$$\frac{H_s}{Hd} = \left(\frac{h_d}{h_s}\right)^{\frac{1}{4}}$$

(4)

Where:

- Hs: Wave height in shallow water
- Hd: Wave height in deep water
- hs: Shallow water depth
- hd: Deep water depth

The shallow wave approximation done will break down when the longitude (L) decrease considerably near shore and the amplitude of the wave is similar or exceeds the water depth. At this point, where Hs ~ hs, the wave height can be expressed as:

$$H_s = H_d^{\frac{4}{3}} \cdot h_d^{\frac{1}{5}}$$

(5)

A 1m height tsunami in the deep ocean (4000m depth) would ends up with a 5m wave height in 5m water depth.

- Refraction

A wave attaining shallower waters decreases its velocity. When the wave front reaches shallower waters indirectly, the wave front in deeper water has a higher celerity. Therefore, when the water depth under a wave varies, the wave has different celerity's along its wave front, and it bends.

Sometimes waves approach with an angle to a straight shoreline. The part of the wave in shallower waters, closer to the coast, moves slower than the part farther from the shore. This behaviour makes the wave crest tend to become parallel to the shoreline (Figure 8).

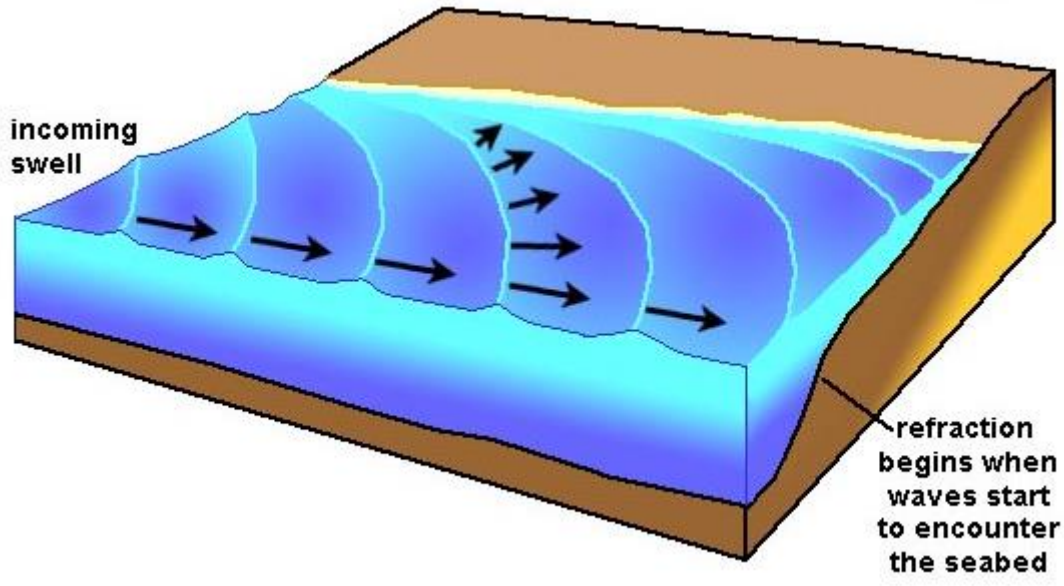

Figure 8: Wave refraction as waves approach the beach at an angle (Oceanography 101, http://gotbooks.miracosta.edu/oceans/chapter10.html).

Tsunamis are shallow water waves even in great depths. The depth in different parts of tsunamis might be widely varying over their wavelengths. Because depth determines the velocity, different wave parts will travel with different velocities, causing the waves to bend. In Figure 9 we see the refraction taking place in waters of great depth too, determining direction changes on the tsunami.

Because of refraction, shore bathymetry may focus the wave energy in shallower coastal areas foreland, as shown in Figure 10.

- Diffraction

Diffraction takes place when the wave height in some point is higher than the adjacent in the same crest. Energy is transferred from the higher point to the lower. If the wave reaches a barrier (island, breakwater) there will be a shadow zone. Diffraction may transfer energy from the wave that hasn´t meet the barrier to the shadow zone. The wave will bend after passing through a gap and spread around the obstacle.

Because of diffraction a tsunami will bend to arrive to shadow zones, as in Figure 9 when the tsunami propagates over the Atlantic Ocean and propagates inside harbours.

When one of the mechanisms that trigger a tsunami (e.g. earthquake) occurs a train of waves is generated and propagated in both sides' directions from the source mechanism. This propagation is generally radial, but if the seismic slip front is longer than hundreds of kilometres, as in the 2004 Indian Ocean Tsunami, the wave could be

strongly directional, propagating much further and preserving the energy relatively unchanged.

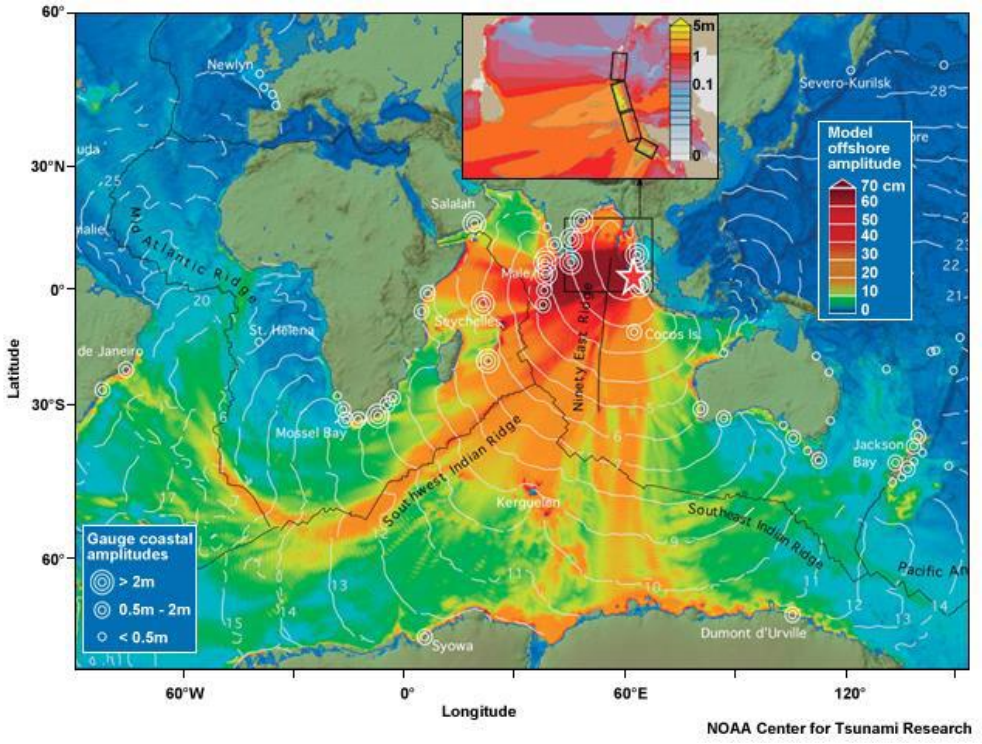

Figure 9: 2004 Indian Ocean Tsunami propagation (NOAA Center for Tsunami Research, 2004).

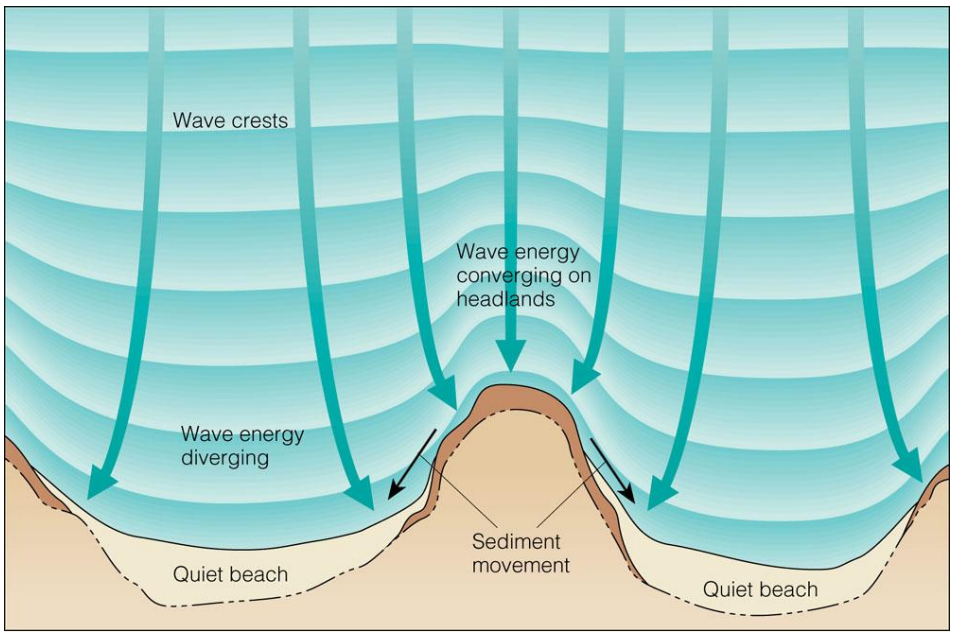

Figure 10: Waves convergence because of refraction. Continuous lines parallel to the coast represent the bathymetry of the area and continuous lines with and arrows represent the direction of wave propagation (Brooks/Cole – Thomson, 2005).

In less than a day, tsunamis can travel from one side of the Pacific to the other. However, people living near areas where large earthquakes occur may find that the tsunami waves will reach their shores within minutes. Tsunami can propagate led by either a depression (trough) or a crest. In the first case the sea shows a recede from the coastline before the positive crest reaches the shore (Rossetto et al., 2011). The source mechanism will define the leading wave characteristics. When the tsunami reaches the coast, it may appear as a fast rising or falling tide.

2.4 Effects of the tsunamis

Small tsunamis, most of them undetectable without specialized equipment, happen almost every day. Nearly all these tsunamis are triggered by minor earthquakes and are too small when they hit the coast to have any significant effect. Often small tsunamis are confused with strong and fast-moving tides or other long waves like seiches. On the other hand, tsunamis are among the more destructive and deadliest natural disasters.

Talking about natural disasters we have to underline the difference between hazard and risk. In earthquakes, the hazard characterises the level of expected ground shaking (acceleration, velocity or deformation), and it is directly related with the tsunami hazard, dependent on the earthquake characteristics. The risk, in the other hand, is the possibility of life and economic losses by the earthquakes or tsunamis.

The hazard takes into account the number, the magnitude and the location of earthquakes in the study area. The areas with a higher strong event frequency have a higher hazard. The hazard depends on the seismic activity and it is evaluated from previous events. Recording earthquakes using seismic monitoring networks is a recent practice, typically done in the last forty years. This data is not representative of long-term activities, so it has to be improved with information from historical writings and from geological studies.

The risk relates de hazard with the vulnerability of an area, being dependent of both. If the hazard is high, but there is no human activity in the area, the human risk is low. The seismic risk can be modified, reducing it with earthquake-resistant constructions.

The effects of a tsunami depend on the wave's characteristics, defining the hazard, and the affected area, defining the vulnerability. Tsunamis have long period and, except for the largest tsunamis, the approaching wave does not break and makes landfall as a forceful rapid increase in the water level. Most of the tsunamis appear like an endlessly onrushing tide. The effect of a tsunami in the coast can be defined by two factors, run-up and inundation.

- Run-up:

  Run-up is the water elevation inland above the normal sea level during the tsunami event. In the largest tsunamis the water level can rise many meters.

  The first wave in a tsunami train does not always produce the highest run-up. The tsunami's frequency combined with some bathymetries can result in resonance and

send more water onshore. Sometimes more than one earthquake or a landslide take place at the same moment and produce two different waves. These waves can meet during the propagation and be combined in a more energetic wave.

The coastal topography has a big influence on the wave run-up. Flat shorelines offer little resistance and allow the wave to go inland easily, giving a short run-up. Steep shorelines, walls or cliffs will force the wave up, giving a higher run-up.

- Inundation

The inundation is the distance the wave travel inland in its horizontal measure. As with the run-up, the shoreline topography highly influences the inundation distance. The relation with the local topography is the opposite of the run-up height, being bigger the inundation in flat shorelines and vice versa.

Tsunamis will have different effects in the area depending on its socio-economic characteristics. In populated areas could cause important human, environmental and economic losses.

- Deaths
  The worst effect of a tsunami is the human life cost. Since 1850, tsunamis have produced more than 430,000 casualties. Usually the little warning time before the tsunami hits the seashore makes very difficult to execute an effective evacuation plan. People living in the coast have no time to escape. The violent force of the tsunami results commonly in death by drowning. Buildings collapsing, electrocution, explosions from gas and floating debris are another cause of death due to tsunamis.

- Diseases
  The areas inundated are flooded with sea water, damaging sewage and fresh water supply infrastructures. Flooding and water supply contamination can spread diseases in the affected area, causing more deaths.

- Environmental impacts
  Tsunamis have a huge impact on animals, plants and natural resources. Tsunamis change the landscape; solid waste and debris are spread, trees and plants are uprooted and animal habitats are destroyed. Land animals die by the same reasons as people, and sea animals die by water pollution. Salted water and other chemicals, affecting the soil fertility, contaminate water and soil. If nuclear power plants are damaged by the tsunami, as it happened in the 2011 Japanese tsunami, there may be radiation spread near them.

- Economic costs
  Tsunamis cause massive costs in the communities and countries affected. Reconstruction and clean-up have big costs. Infrastructures must be replaced, unsafe buildings demolished and debris cleared. In non-developed countries buildings and infrastructures are not prepared and cannot withstand the impact

of a tsunami. Whole areas and towns can be completely destroyed as the tsunami leaves as trail devastation and misery behind it.

Papadopoulos and Imamura (2001) introduced a new 12-point tsunami intensity scale to classify them. The scale considers the effects on humans, on objects and on nature and damage to buildings, where I correspond to “Not felt” and XII to “Completely devastating”.

For a better understanding, it is necessary to know the relation between the event characteristics and its effects. The last great tsunamis, as the 2004 Indonesian and 2011 Japanese tsunamis, have provided a big amount of data useful to improve our knowledge about tsunamis and its effects.

- 2004 Indian Ocean tsunami.

In December 2004 a magnitude 9.1 earthquake produced a destructive tsunami in north-western Sumatra, Indonesia. It has been the deadliest tsunami recorded and one of the most destructive natural disasters in history.

The wave strokes the coasts throughout the Indian Ocean, causing 228,000 casualties, displacing more than one million people and causing billions of dollars of property damage. The wave reached 24m run-up, rising to 30m in some areas when travelling inland.

The Belgian yacht “Mercator” recorded the free surface elevation after the earthquake occurred. The yacht was anchored 1 mile (1.85km) off Nai Harn Bay, in the southwest of Phuket, with 12m water depth below it (Grilli et al, 2007). The depth echo sounder in the Mercator recorded the free surface elevation over the first two hours of its propagation (Figure 11).

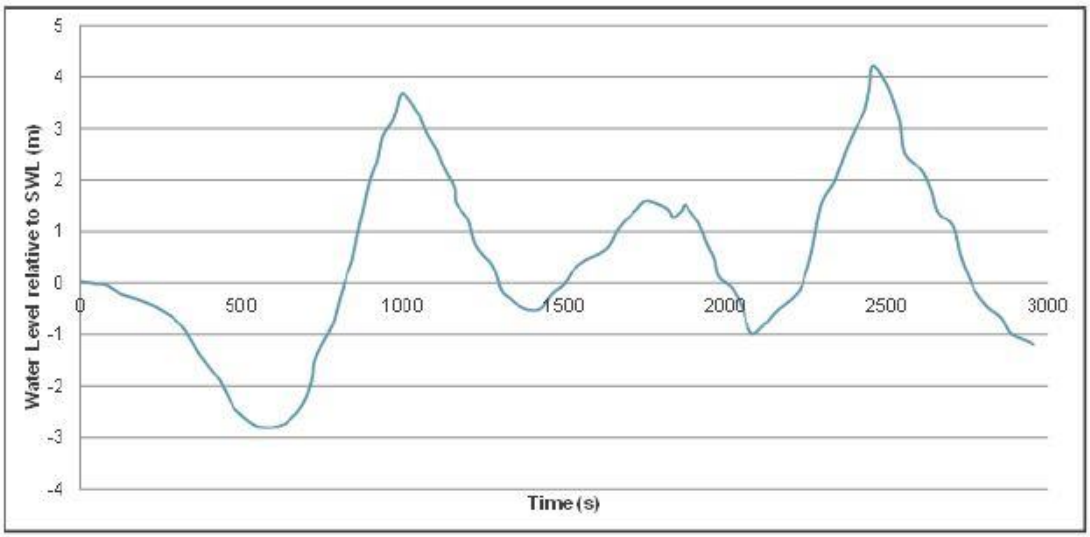

Figure 11: Signal recorded by the Mercator yacht (Chandler et al., 2016).

- 2011 Japanese Tsunami

On 11th March 2011, a magnitude 9.0 earthquake generated a giant local tsunami in Japan. The National Police Agency of Japan confirmed the wave claim nearly

16,000 lives, more than 6,000 people were injured and 2,500 people are missing in Tohoku, Japan.

The pressure gauges recorded the sea level that followed the seismic event (Figure 12 and Figure 13). We can see no trough was registered. The wave increases in two steps, a first 2m crest followed by a total 5m crest, and then goes back to the initial condition in similar steps.

Groups of researchers from throughout Japan conducted a tsunami survey along the Japanese coast. The maximum run-up measured was 40.5m, and the wave reached more than 5km inland (Mori et al, 2011). The tsunami inundated approximately 561km2 in Japan. Figure 14 shows the wave arriving Miyako City, in the Japan northeast.

The damage in the Japanese structures and infrastructures was considerable. More than 45,000 buildings were destroyed and around 144,000 were damaged (Figure 15). Fifteen ports were located near the disaster area. Four of the north-eastern ports were destroyed and other two were affected, though less severely. Eight more Japanese ports were damaged and closed to ships.

The Fukushima Daiichi and other three nuclear power stations were automatically shut down after the earthquake. However, the tsunami waves overtopped Fukushima Daiichi and Daini seawalls. Diesel backup power was destroyed by the tsunami, leading to severe problems at Fukushima Daiichi. Three explosions took place, leaking radioactive material. Recent studies found that many Japanese nuclear stations were not protected properly against tsunamis (Philip et al., 2013).

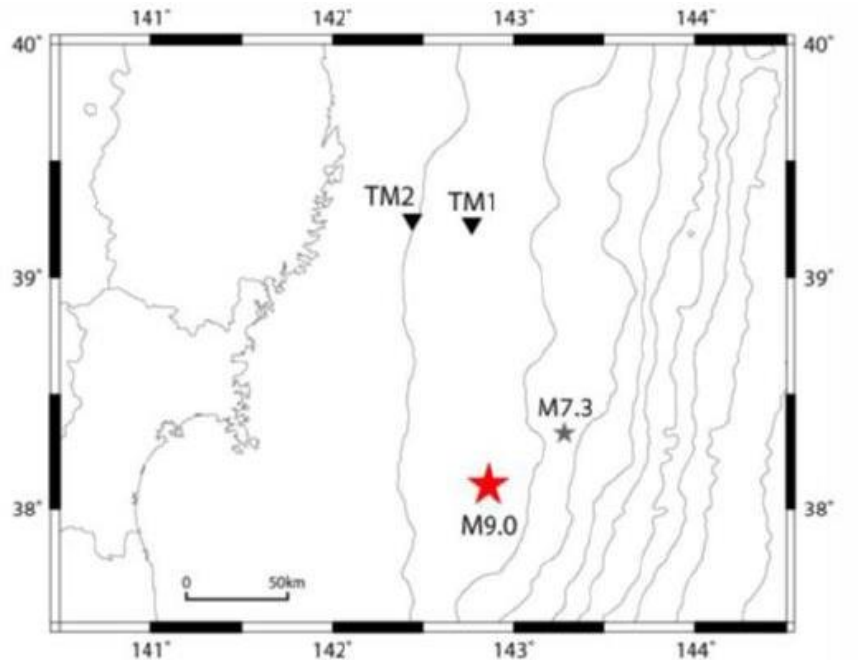

*Figure 12: Location of the Ocean Bottom Pressure Gauges TM1 and TM2 and location of the estimated epicenters (*Earthquake Research Institute of Tokyo University, *http://www.eri.u-tokyo.ac.jp/en/)*.

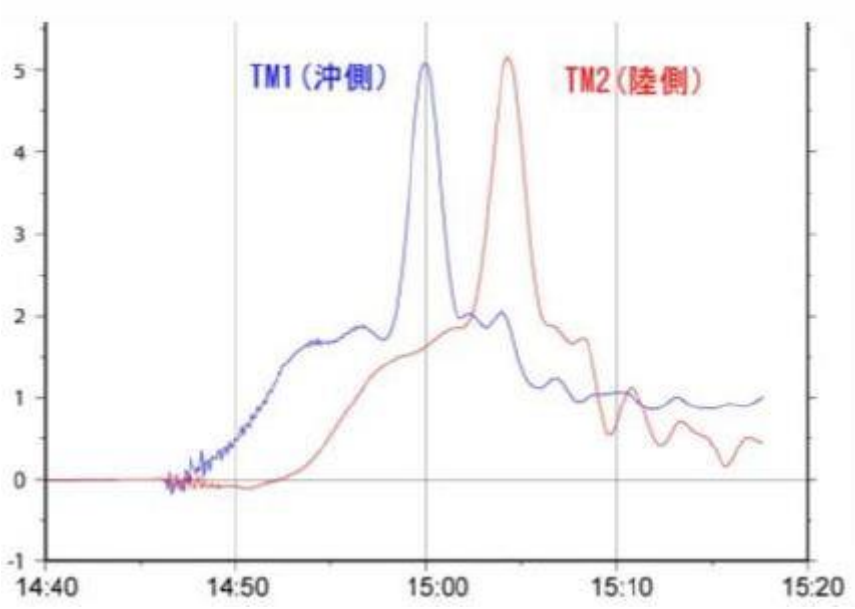

Figure 13: Free surface elevation (m) records from the *o*cean *b*ottom *p*ressure *g*auge 11 March 2011 *(*Earthquake Research Institute of Tokyo University, *http://www.eri.u-tokyo.ac.jp/en/)*.

Figure 14: The tsunami wave approaches Miyako City from the Heigawa estuary in Iwate Prefecture (Mamarantau, 2011).

Figure 15: Smoke rises in the distance behind destroyed houses in Kesennuma City (Mamarantau, 2011).

2. Earthquakes and tsunamis in the Mediterranean Sea

The Mediterranean region is characterized by successive, connected Neogene fold-and thrust belts and associated foreland and backarc basins. Over this area, Tethys oceanic lithosphere domains, originally present between Eurasia and African-Arabian plates, have been progressively subducted (e.g. Cavazza et al., 2004). The systems are typically characterized by arcuate, narrow compressional zones and extended basins with a distribution of relief and morphologies that roughly resemble each other across the Mediterranean.

Until recently it has widely believed that tsunamis did not occur in the Mediterranean Sea, or they were a strange phenomenon that hardly could threaten coastal areas (Papadopoulos and Fokaefs, 2005). However, moderate to high seismicity and a considerable volcanism characterize the geodynamics of the Mediterranean Sea. In addition, coastal and submarine landslides are not strange. Thus, even if the

Mediterranean Sea constitutes only the one percent of the World ocean water, ten percent of all tsunamis reported worldwide have occurred in it. On average, one disastrous tsunami takes place in the Mediterranean region every century. Geological research and historical records report many powerful tsunami events that have taken the lives of thousands over the ages.

3.1 Earthquakes in the Mediterranean Sea

The Mediterranean Sea region shows a remarkable seismic activity because its location in the boundary between major tectonic plates (cf. section 1.1). Two of the major tectonic plates meet on the Mediterranean Sea, the African plate and the Eurasian plate. To the east the Mediterranean Sea is bounded by three minor plates, the Arabian, the Aegean, or Hellenic one, and the Anatolian plates (Figure 16).

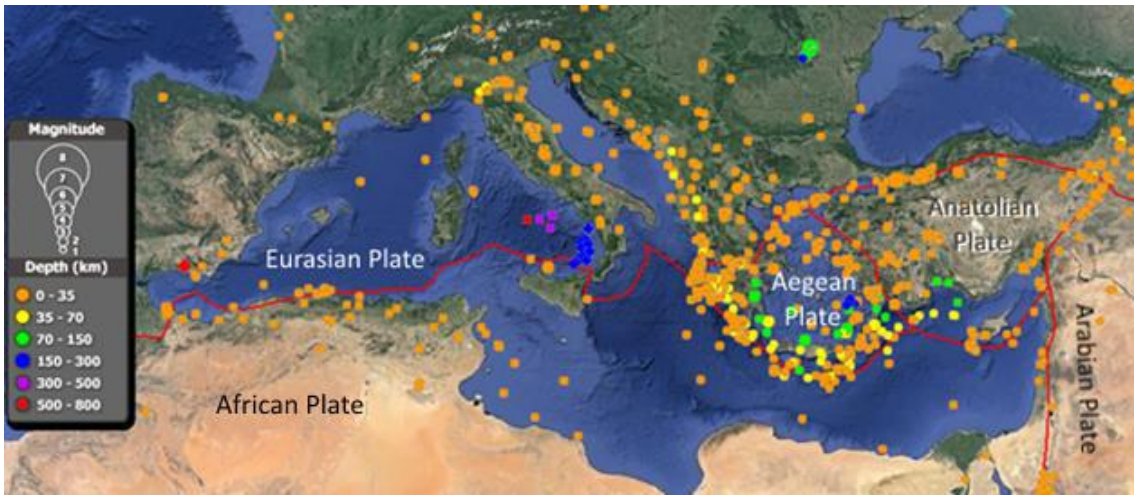

Figure 16: Mediterranean tectonic plates and earthquakes with magnitude 5.0 or bigger between 1983 and 2012, plotted by depth (Google Earth & On the Cutting Edge: Professional Development for Geoscience Faculty, https://serc.carleton.edu/NAGTWorkshops/visualize04/tool_examples/google_earth.html).

The mapped seismicity shows a remarkable activity near the plate boundary between African and Aegean plates. In addition, there is also noticeable seismic activity along northern Africa margin (Magrheb), Italy and the Balkans coast. The source of some of those earthquakes is located at sea and could trigger tsunamis in the future.

The Mediterranean seismic hazard map (Figure 17) shows the earthquake hazard level over the area, evaluated from the recorded historical and instrumental seismic activity. In this map it can be observed that the Aegean Arc localizes a high number of earthquakes and is the source of the major events happened in the Mediterranean Sea. The largest shallow earthquake measured in the twentieth century on the Aegean Arc had reported magnitudes around 7.2. There are historical sources and geologic and archaeological studies suggesting larger earthquakes, around magnitude 8, with epicentres near Crete occurred in the 365 AD and 1303 AD. Both earthquakes triggered devastating tsunamis along the Mediterranean coasts. In 1956 a magnitude 7.8 earthquake in the south of Amorgos produced a large tsunami in the Aegean Sea. In the

region shallow focus earthquakes are also caused because of volcanic activity, as in the Dodecanese and Cyclades Islands, 100km north of Crete.

Many earthquakes take place at the Calabrian Arc, being the 1908 Messina earthquake the most devastating. This earthquake produced a tsunami, adding more destruction to the generated by the earthquake.

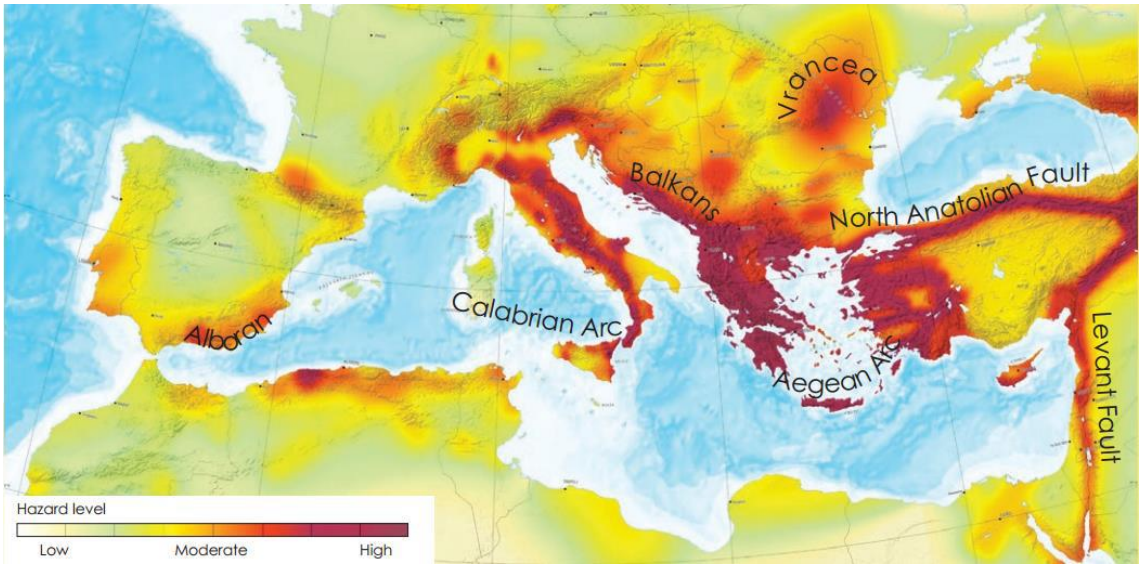

Figure 17: Seismic hazard map of the Mediterranean area (Modified from © ESC-SESAME, 2003).

3.2 Tsunamis in the Mediterranean Sea

In the Mediterranean Sea up to four tsunamis have been classified as degree X in the intensity tsunami scale:

- 365 Crete tsunami:

  On 21th July 365 an estimated magnitude 8 offshore earthquake occurred near Crete caused the destruction of nearly all the cities in the island and triggered a tsunami (Stiros, 2010). The tsunami spread until the coastal regions of Egypt and Sicily, causing destruction all over the Mediterranean Basin.

  Records describe the tsunami hitting Alexandria like a trough leading wave and indicate that 50,000 people lost their lives only in this city.

- 1303 Crete tsunami:

  Another estimated magnitude 8 earthquake struck the island of Crete on 8th August 1303. The earthquake destroyed the city of Rhodes and part of Crete. The generated tsunami reached Alexandria city in the Egyptian coast. Numerical models estimated a 9m run-up at the Alexandria area (Papadopoulos et al., 2007).

- 1650 Santorini tsunami:

A submarine explosion from the Kolumbo Volcano on 26th September 1650 generated a tsunami killing 70 people in the Santorini coast. Waves up to 16m stroke the island of Los, north of Santorini (Dominey-Howes et al., 2000).

- 1908 Messina tsunami:

On 28th December 1908 an earthquake and the triggered tsunami caused over 128,000 casualties in Sicily and Calabria, south of Italy. The cities of Messina and Reggio Calabria were highly affected and close to be completely destroyed (Pino et al., 2008).

More concretely in the Region that covers the coasts of Algeria, Balearic Islands and the Spanish coasts facing the Alboran Sea, the majority of the 13 events were generated by the Tell-Atlas thrust system, which accommodates a significant portion of the Africa-Europe convergence in the western Mediterranean and is capable of generating strong earthquakes and trigger basin wide tsunamis (Aoudia and Meghraoui 1995, Aoudia et al. 2000, Meghraoui et al. 2004). The Black Sea region includes the Crimean coasts.

The last tsunami registered in the Mediterranean Sea took place on the 21th of May 2003, in the Alboran and western Mediterranean Sea. The tsunami, assigned with intensity IV, hit the Algerian coast and the Balearic Islands and caused a great amount of economic losses in the archipelago.

Figure 18 shows a map of the known tsunamigenic sources in the Mediterranean Sea and a relative scale of the tsunami hazard. The potential for tsunami generation has been calculated as a convolution of occurrence frequency and intensity of the tsunami events. These data are valid as long as tsunami records over the last centuries could be extrapolated to longer time periods. The long return period that characterize tsunamis in some tsunamigenic zones and the lack of data diminish the confidence in the recurrence for strong events. Therefore, the average recurrence of 140 years for the very strong events should be regarded as an “apparent” mean repeat time (Papadopoulos, 2005).

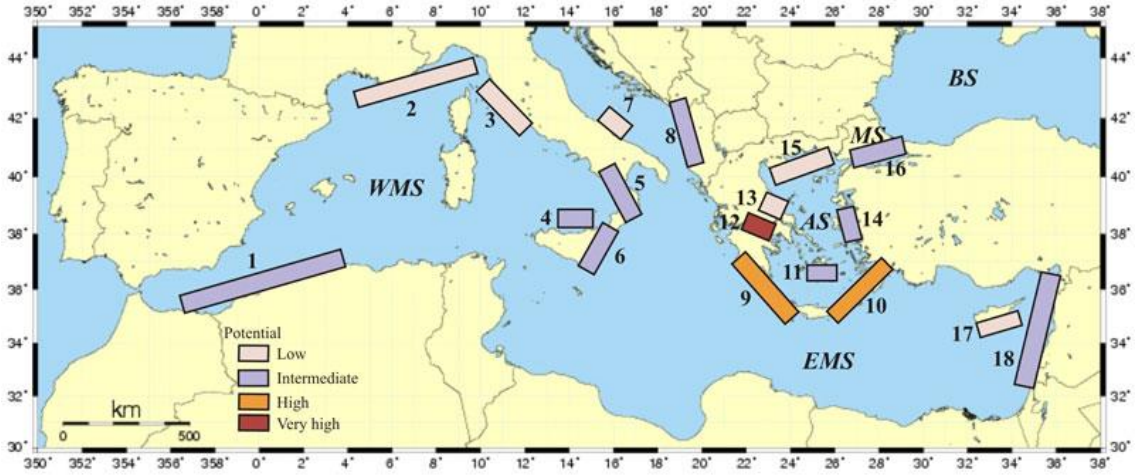

Figure 18: Tsunamigenic zones of the Mediterranean Sea. Source: (Papadopoulos, 2005).

3.3 The Balearic Coast

The Balearic coasts are exposed to earthquake-generated tsunamis from the North Africa margin, particularly from Algeria. In fact, along the coastal strip between Colònia de Sant Jordi and Cap de Ses Salines, extensive ridges made of large imbricate blocks up to ~24t in weight and 5x3x1 m in size are viewed by some as evidences of paleo-tsunamis deposits. Investigating such shallow environments in search of tsunami impact evidence is a challenge by itself, as this is a fringe impacted by regular high energy marine processes (i.e. storms) that tend to remove any sedimentary evidence of tsunamis except eventually for very large boulders and parent erosional surfaces.

Also, all the south-east coast and part of the east coast have boulders up to 3.20x2.50x1 m in size and of an estimated weight of 8t (Figure 19) as the top boulder of the figure 3.4.

Figure 19: Imbricated boulders in the east coast of Mallorca, Cala Mitjana.

In contrast, deposits left inland by tsunami run-out at varying distances from the shoreline are relatively common and are widely used by paleotsunami research (Figure 20). It should also be mentioned that the tsunami resulting from the 2003 Boumerdes earthquake in Algeria hit the Balears in the late evening of the 21th of May sinking 200 boats despite the maximum run-up was slightly over 1 m.

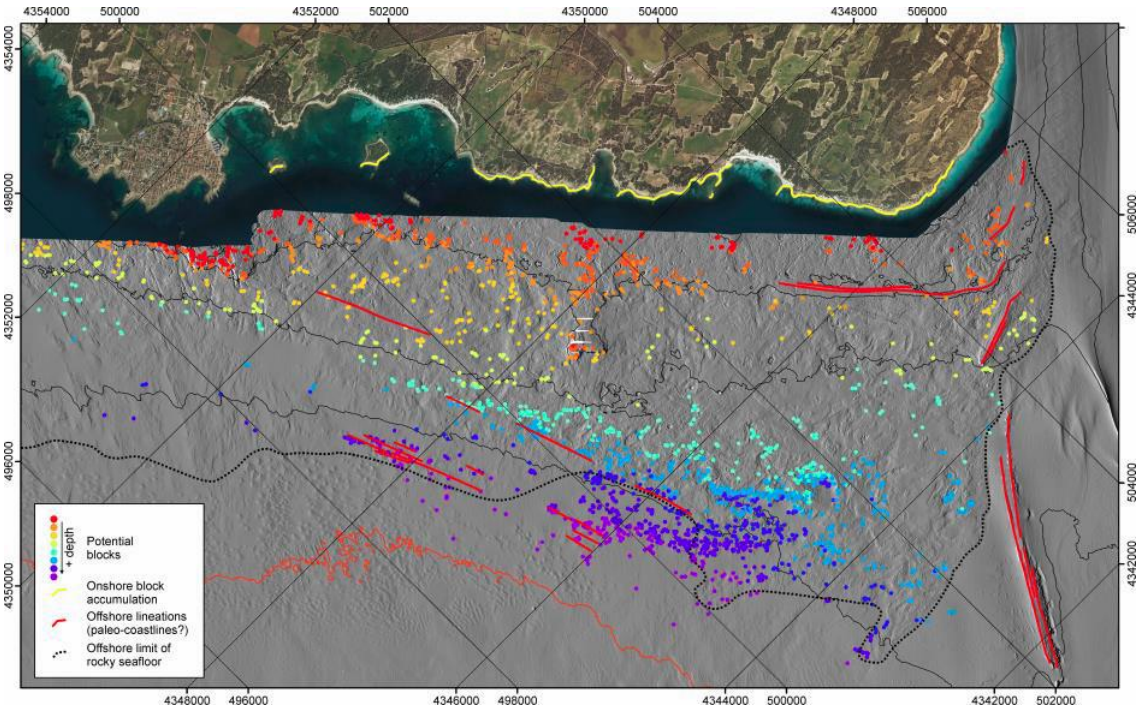

Figure 20: Potential large boulder on the innermost continental shelf between Colònia de Sant Jordi (left) and Cap de Ses Salines (rigfht). Note that most boulders are aligned following given depth ranges (red to violet colours). North is towards the upper left corner of the image (ASTARTE project, 2014).

3.4 The ASTARTE project

The ASTARTE (Assessment, STrategy And Risk Reduction for Tsunamis in Europe) project summarizes the work carried out and the results achieved on the identification of mass transport deposits (MDTs) and other deposits that could have been caused by tsunamis in the North-Eastern Atlantic, Mediterranean and Connected Seas (NEAM) region. Such work replies on sediment cores and other direct sedimentary evidence, and on geophysical datasets such as high-resolution seismic reflection profiles and multibeam bathymetry maps.

The work performed embraces a large variety of tectonic and sedimentary settings, ranging from shallow subaqueous deltas and innermost continental shelves to open shelves, continental slopes, deep basins and seamounts, both in the Mediterranean Sea and in the North-East Atlantic Ocean.

Whereas the identification of classical MTDs (i.e. turbidites, landslides deposits and other deposits resulting from mass transport processes) poses few difficulties thanks to their distinct character, their direct attribution to tsunamis is more challenging, as MTDs

may result from a variety of processes that do not necessarily involve tsunami generation. Less known sedimentary evidences of possible past tsunamis, such us accumulations of meter-sized, eventually imbricated boulders, on the innermost shelf or thin “anomalous” layers on the continental shelf have been investigated too.

Clusters of metric-sized boulders on the innermost shelf, “anomalous” layers on continental shelves and deep-water turbidites/homogenites and landslide deposits of varying characteristics have all been investigated within ASTARTE at key locations within the NEAM region, thus providing a comprehensive vision of the offshore record of MTDs in the marine basins of Europe, some of which are clearly linked to tsunamis. Where numerous, well-dated events have been identified, indicative recurrence rates have been estimated. These rates show that although not highly frequent if viewed against the duration of a normal human life, tsunamigenic processes and resulting tsunamis can impact almost every place along the shores of Europe as demonstrated by widespread evidence of MTDs and other deposits directly related to past tsunamis (Baptista).

3.5 Tsunami indicators: boulders and Transport Figure (TF) in the Balearic Islands.

More than 4.000 boulders are registered in the Balearic Islands. Some have been dated by Bartel and Kelletat (2003), Kellet et al. (2005) and Schefers and Kelletat (2003). Folloeing Roig-Munar et al., (2016), there is a Transport Figure equation based on Scheffers and Kletat (2003)(Figure 22). The equation is based on the highness of the boulder about the level sea, the weight and other aspects. In their paper Roig-Munar et al. (2016) consider a Transport Figure > 1000 as indicator of tsunami-transported boulders, which is more than four times above that considered by the previous authors.

Roig-Munar et al., (2016) estimate the weight of the boulders like a normal volume formula, base by height by depth, or defining the axes a, b, c. And then, he multiplies by 0.3, like a porosity index. In our study zone, the same will be done.

The fact that the disposition of the boulder repositioned by tsunamis and by storms are different is understandable by just seeing the focus of the tsunamis, figure 23. As it can be seen, the main focus is in the Algerian coast so, the zones that are orientated to the north in the Balearic Islands, are more protected than the south zones.

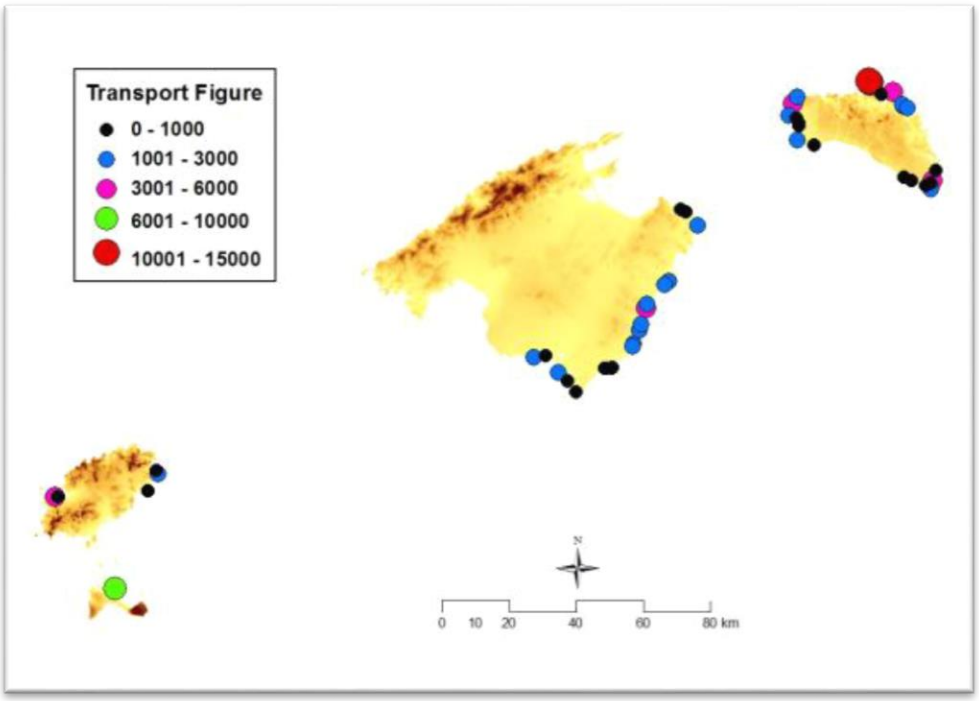

Figure 22: Transport Figure values (Roig-Munar et al., 2016).

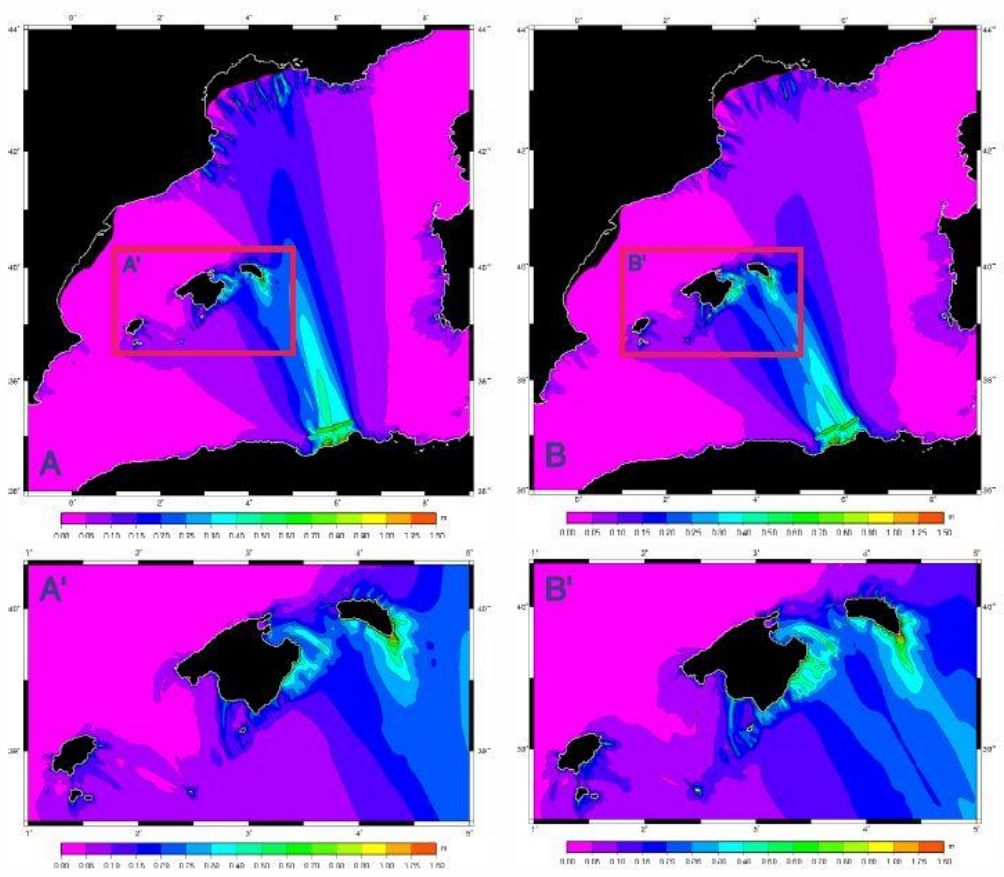

Figure 21: Maximum wave heights cumulated on 1.5 h after the rupture involving the 3 segments simultaneously, with a mean strike of 80 (left, A and A') or 60 (right, B and B') (*Roger* and *Hébert,2008).*

3.6 MTDs in the Mediterranean Sea

Tsunamis were historically reported to have been also generated in association to aseismic processes usually with the involvement of coastal and/or submarine landslides. In fact, the continental margins in the Mediterranean Sea favour such processes since they are steep, narrow, usually fed by small mountain-supplied rivers and as a rule controlled by tectonic activity. A long number of scars and mass-failure deposits have been reported to occur in both tectonically active and quiet areas and at sea depths ranging from very shallow up to 2 km (e.g. Camerlenghi et al., 2010; Urgeles and Camerlenghi, in press.). The volumes of continental-slope deposits remobilized range from less than 0,001 km3 to more than 1,000 km3 while their ages fall in the time interval from the last 100,000 years to very recent times. Mass failures processes are of particular importance as regards their potential for the initiation of tsunamis.

Submarine landslides are ubiquitous on the Mediterranean margins of the Western Mediterranean and the adjacent SW Iberian Margin. Available marine geophysical data evidence complex slope failure systems, although understanding the distribution of known submarine landslides is not straightforward because of incomplete coverage and lack of uniform studies in all areas (Camerlenghi et al., 2010; Urgeles and Camerlenghi, in press.). Nevertheless, during the last two decades, improvements in swath mapping and geophysical techniques allowed to identify hundreds of submarine landslides. In the western Mediterranean, most failures have limited volume, short runout and originate in relatively deep water. Therefore, only the largest albeit infrequent events are likely to trigger large tsunamis. The so-called BIG'95, with a volume of 26 km3 and 110 km runout (Lastras et al., 2002; Urgeles et al., 2007), is one of such events in the Western Mediterranean basin (Løvholt et al., 2009; Tinti et al., 2009; Iglesias et al., 2012). Seismicity is a major control in the distribution, magnitude and typology of submarine landslides (Camerlenghi et al., 2010; Urgeles and Camerlenghi, in press), but other factors, mainly fluvial sediment input and margin progradation (Field and Gardner, 1990; Lastras et al., 2007), come to play an important role too.

In the easternmost Mediterranean basin, the main source of recent sedimentation is the Nile river. Most of Nile's load was deposited in its delta and a significant portion was conveyed further NW-wards, offshore along the Levant continental margins (Stanley, 1989). Such young, soft and unconsolidated materials are vulnerable to voluminous gravitational collapses (e.g. Frey-Martinez et al., 2005; Garziglia et al., 2008; Folkman and Mart, 2008). According to Rosen (2011), landslides may also occur due to scouring of the lower part of the eastern flank of the Nile delta unconsolidated sediments. Further to the east, in the Levantine Sea, there is substantial evidence for submarine slump complexes off the coast of Israel and Lebanon (e.g. Frey-Martinez et al., 2005, Salamon et al., 2009). In Central Greece, the predominant structure is the rift of Corinth Gulf (e.g. Armijo et al., 1996, Moretti et al., 2003) which is also characterized by high seismicity and is typical for local tsunamis triggered by both earthquakes and coastal/submarine landslides (e.g. Papadopoulos, 2003, Lykousis et al., 2008).

3. Creation of a synthesis GIS map

The synthesis GIS map created in this thesis is available here: https://drive.google.com/drive/folders/1aeRkDXvCuPtYKztlU9fib_OfAFkk89KK?usp=sharing. The MarMediterrani.mxd file is done with the ArcMap v10.4 and the MarMediterrani1.mxd is done with the ArcMap v10.3.

4.1 The Mediterranean outline shapefile (MedSea.shp and OutLine.shp)

To begin the creation of the Mediterranean Sea basin, the separation between the coast and the sea, we have searched a shapefile for the posterior clip to our study zone. In the web side of Marine Regions (http://www.marineregions.org/downloads.php#iho) we have found a shapefile of lines that embeds all the coasts (Figure 24). The clip has been necessary because it was bigger than the study zone and for the clip features a rectangular shapefile "OutLine.shp" has been created, including the Mediterranean basin.

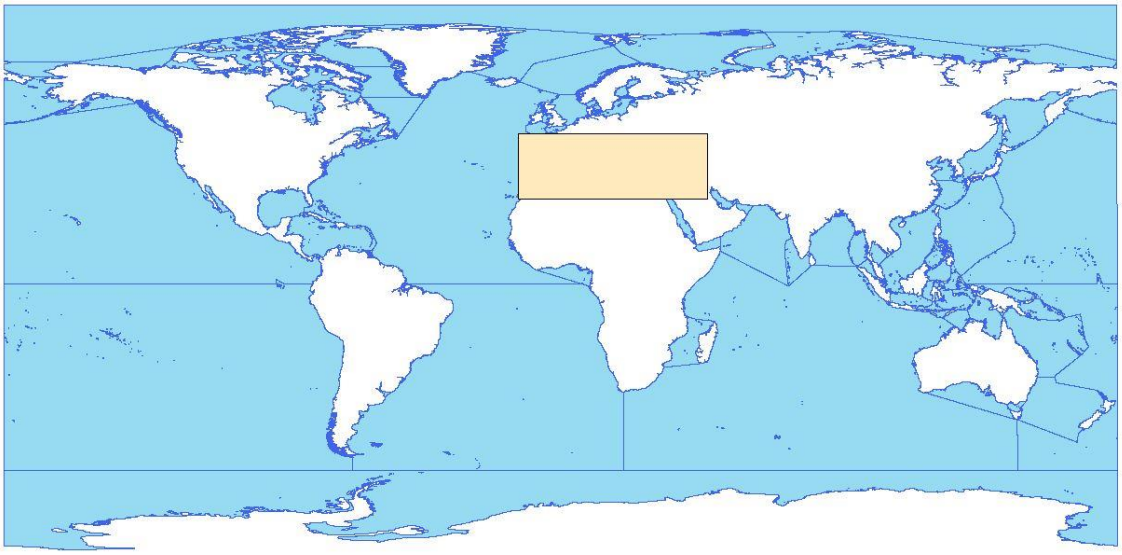

Figure 23: In blue the polygons that conform the seas separating the land. In beige the polygon used to clip the study zone (Marine Regions, http://www.marineregions.org/downloads.php#iho).

Once clipped and overlaid correctly, the outline of the Mediterranean Sea is finished, figure 25.

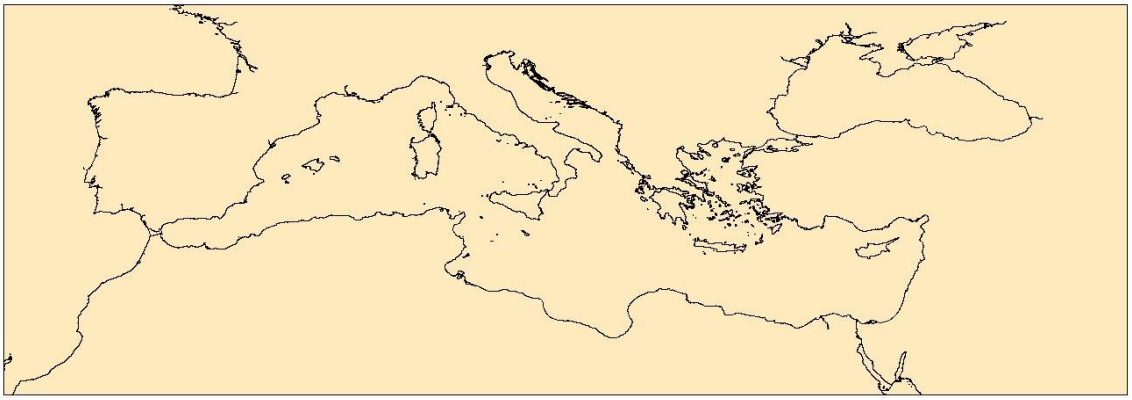

Figure 24: The Mediterranean basin defined. Source zone (Marine Regions, http://www.marineregions.org/downloads.php#iho).

Additionally, some polygons have been merged in order to simplify de basin.

4.2 The Bathymetry DEM (bathymetry)

In the same way the bathymetry has been downloaded, added and merged to the project.

First, six ASC II files have been downloaded from the EMODnet portal (http://portal.emodnet-bathymetry.eu/). Secondly, the ASC II files have been converted to raster files with the "clip" tool, figure 26. Then, with the "Mosaic to new raster" tool the rasters have been merged for simplicity and smooth the borders between the maps. The colour ramp has been changed too, figure 27.

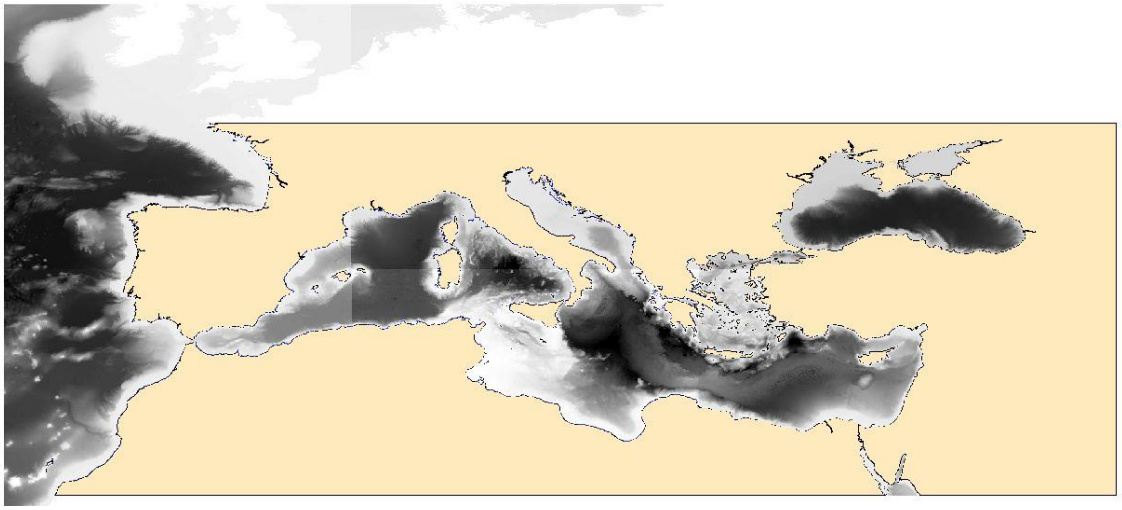

Figure 256: The ASC II files converted into raster files (EMODnet, http://portal.emodnet-bathymetry.eu/).

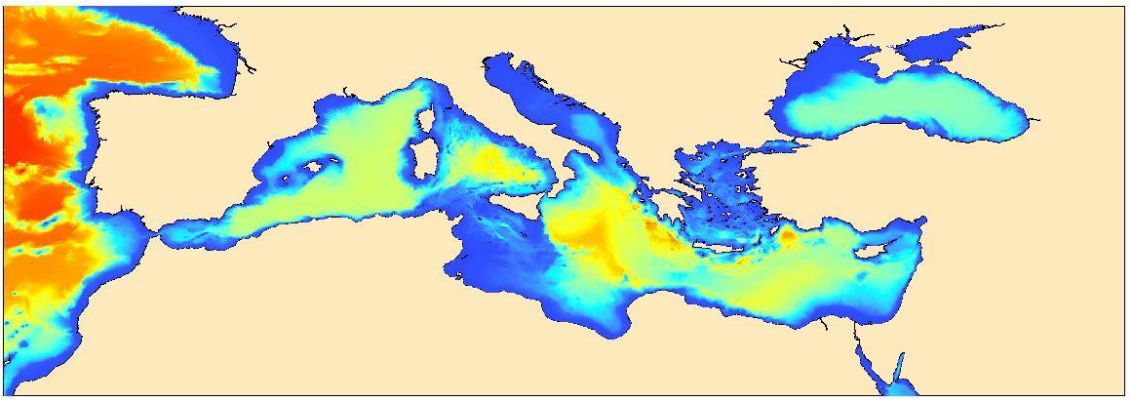

Figure 27: The final bathymetry DEM (EMODnet, http://portal.emodnet-bathymetry.eu/).

4.3 Europe's main coastal cities shapefile (Europe_Cities.shp)

For an easiest view of the hazard tsunamis and future discussions, a shapefile with polygons has been added, figure 28.

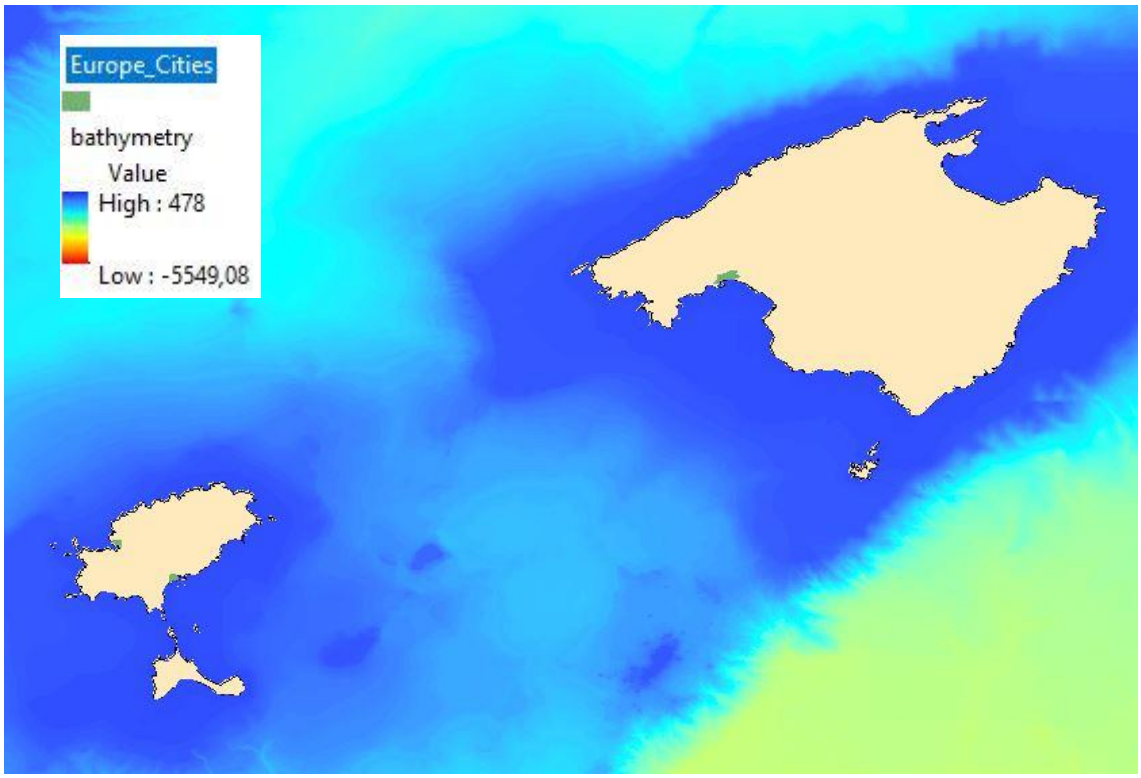

Figure 26: Example of the view of three European cities in Mallorca and Eivissa (Efraín Porto Tapiquén, https://tapiquen-sig.jimdo.com/english-version/free-downloads/europe/).

4.4 The topography shapefile (Contours.shp)

A topography of interest areas like the Balearic Islands has been added to better understand the deposits of paleo-tsunamis. For that, a several number of shapefiles has been downloaded and merged to simplify the GIS map. This data is all from the web site open DEM (http://www.opendem.info/opendem_client.html). The finale layer, "Contours.shp" is the result of merge all the previous downloaded shapefiles.

4.5 The earthquake shapefile (earthquakes.shp)

Most tsunamis are triggered by earthquakes, for correlate which earthquakes or which earthquake zones are the causers of tsunamis is important to put as many tsunamis as possible in one map.

For the earthquakes_isc.shp we downloaded and .scv file from thi ISC web side with more than 1.000 earthquakes and exported as points in the map. Then the same has been done for the USGS and the earthquakes.shp has been created. Once we merged, we obtained a layer of 5.248 tsunamis around the Mediterranean lands, figure 29.

The tsunamis have been classified by his magnitude, in 5 categories.

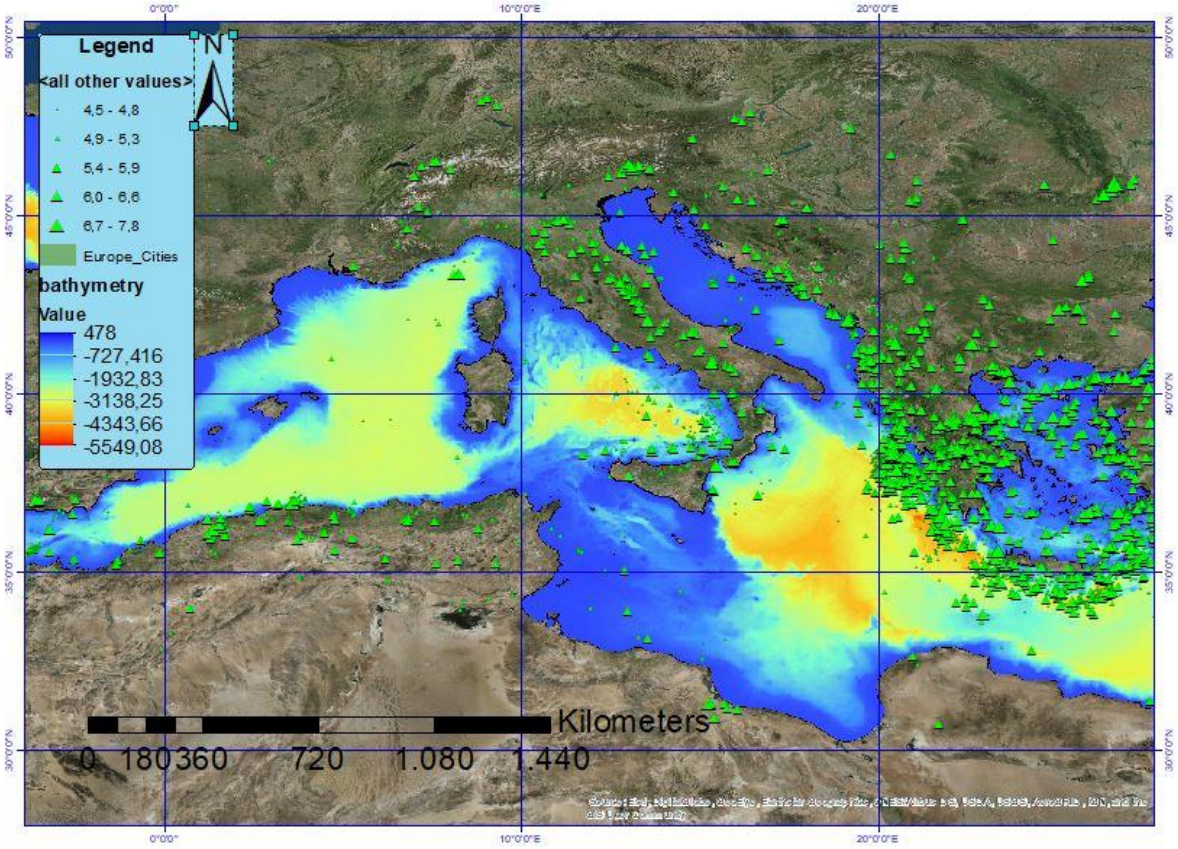

Figure 27: Earthquakes in and near the Mediterranean Basin in green triangles. A satellite base map has been added to put more prespective (ISC and USGS, http://www.isc.ac.uk/iscgem/download.php https://earthquake.usgs.gov/learn/topics/haywardfault/gis/).

4.6 The tsunamis shapefiles (tsunamis.shp)

For the tsunamis layer, The Euro-Mediterranean Tsunami Catalogue has send an .csv file where are a total of 9 earthquakes that have triggered a tsunami. In addition, another shapefile with tsunamis around the world have been downloaded from the USGS page in order to add other tsunamis in the Mediterranean area. Finally, both files have been merged as it can be seen in the figure 30.

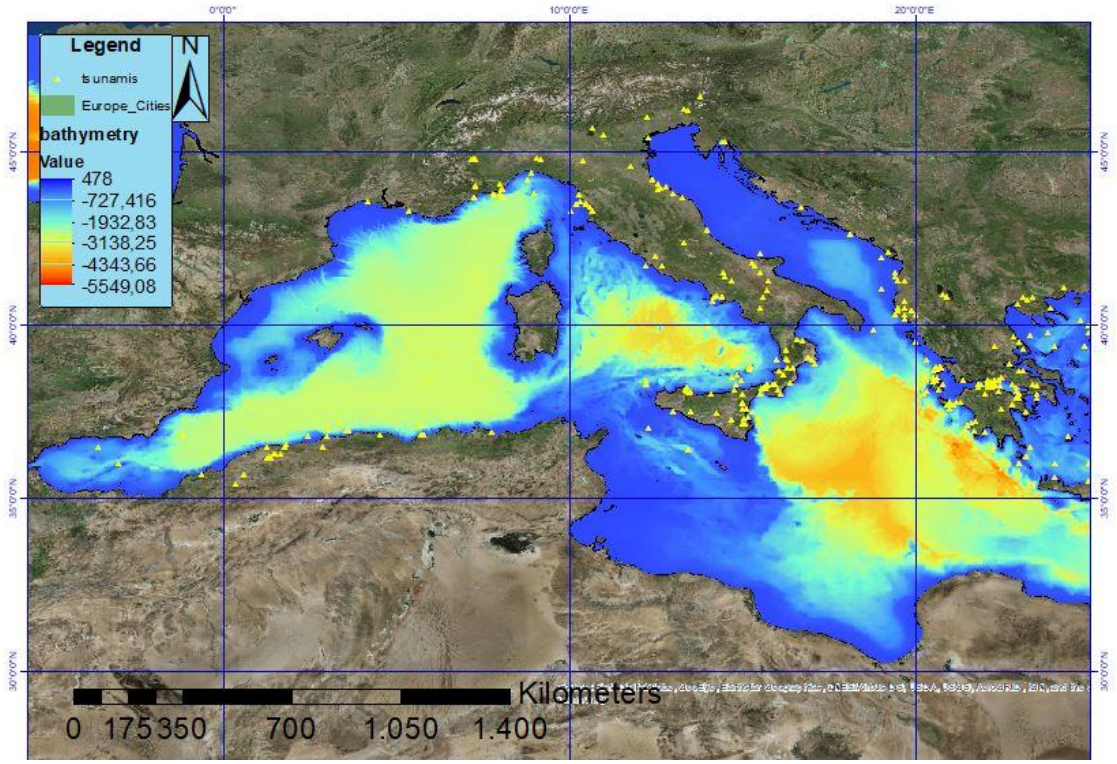

Figure 28: All the earthquakes and that has triggered a tsunami (The Euro-Mediterranean Tsunami Catalogue and USGS, https://www.sciencebase.gov/catalog/item/4f4e4797e4b07f02db48e631).

4.7 The boulder deposits shapefile (boulders.shp)

The boulder deposits layer is a shapefile of points where each point is a zone where are accumulations of boulders placed by tsunamis. The main source of this layer has been taken from "The ASTARTE Paleotsunami deposits database - NEAM region - V. 2017.2" (https://www.arcgis.com/home/webmap/viewer.html?webmap=4eea1187ed1b4ccd889e533b1667e4ab&extent=-72.2569,1.5325,101.3271,72.7755). For that work, an excel have been exported to ArcGis and then saved as a shapefile. The result is in the figure 31.

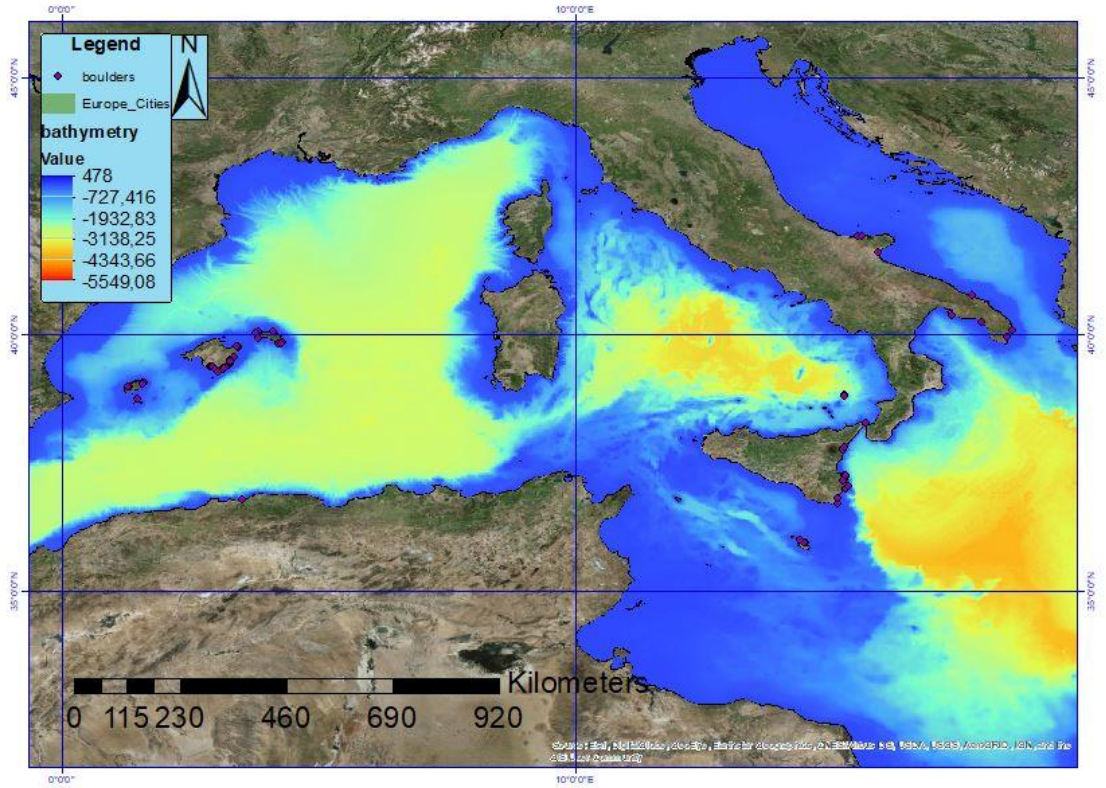

Figure 291: Global view of the sedimentary deposits in the Mediterranean Basin

This layer is also completed with information taken in Mallorca by the author (DepositMall.shp) in the field and using the ASTARTE field trip document of 8th oh april document (Schedule et al.) and the Roig-Munar, F. X., Vilaplana, J. M., Rodríguez-Perea, A., Martín-Prieto, J. A., & Gelabert, B. (2016). Indicadores geomorfológicos de tsunamis históricos en las costas rocosas de Baleares. Geo-Temas, 16(1), 641–644. Docuemtn (depositsMall2.shp). For this, two additional layers have been added to add more deposits as it can be seen in the figure 32.

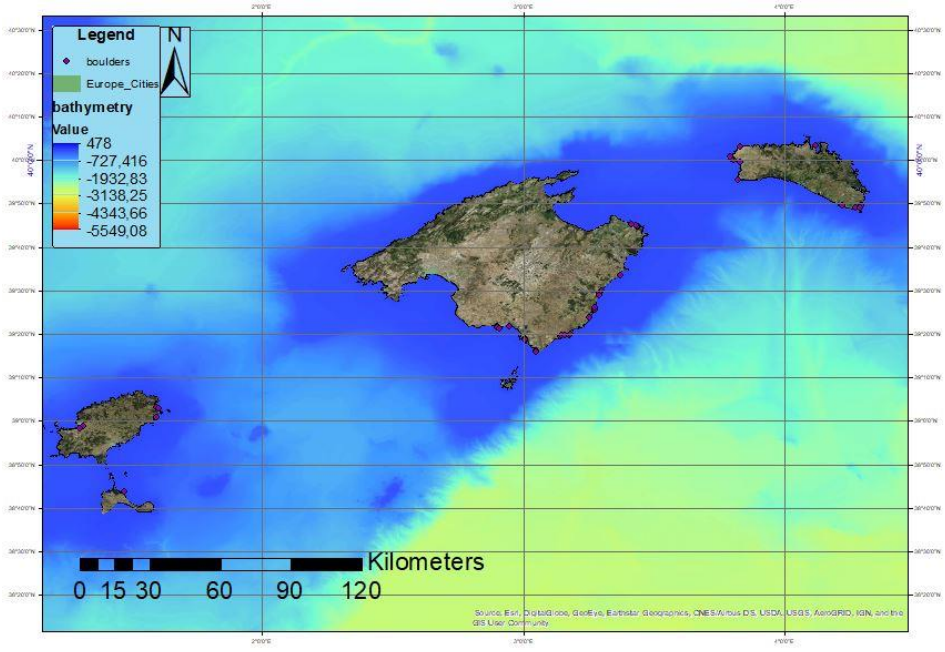

Figure 32: The view of disposition of the boulder generated by tsunamis in Balearic Islands

4.8 The MTDs shapefile (landslide_pol.shp)

The MTDs shapefile have been generated with the work package 6 of the EMODnet portal. Work package 6 “Geological events and probabilities”, led by the Geological Survey of Italy – ISPRA, represents data at 1:250,000 scale as polygons, lines and points. The use of different geometric features is related to the peculiar characteristics of each occurrence, as well as to the scale of representation:

- submarine landslides (lines, polygons, points)
- submarine volcanoes (lines, polygons, points)
- tsunamis origin (points)
- tsunamis affected coasts (points)
- submarine tectonics (lines)
- submarine fluid emissions of non-volcanic origin (polygons, points)

For this work it has just been added the landslides and the submarine tectonics shapefiles. This is because the other layers are not relevant or are already included, figure 33.

For a better vision, a quaternary tectonics layer has been added (quaternary_tectonics.shp).

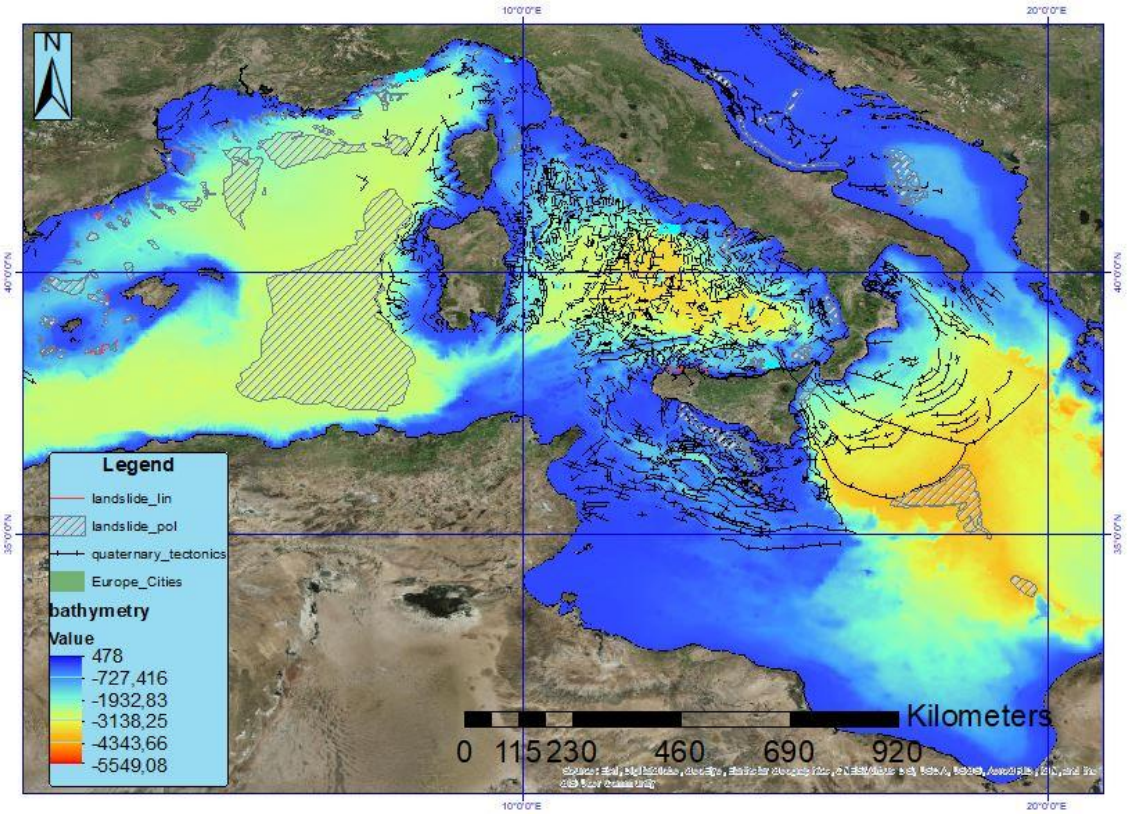

Figure 33: Submarine landsides in the Mediterranean basin (EMODnet portal, http://www.emodnet-geology.eu/data-products/).

4. Field work in Mallorca Island

The Alboran Sea is located on the western end of the Mediterranean Sea. Tectonically, the Alboran Basin is a complex zone that is being squeezed between the approaching Iberian and African plates. This convergence between the two main plates deforms the Alboran thinned crust, forming a set of conjugate shear zones and transpressive structures, including reverse faults, active since the Late Tortonian (Larouzière et al., 1988; Bourgois et al., 1992; Comas et al., 1992; Vegas, 1992; Woodside and Maldonado, 1992; Watts et al., 1993; Martínez-Díaz, 2002; Masana et al., 2004; Gràcia et al., 2006). Although the rate of deformation is low, approximately 4.7 mm/year (McClusky et al., 2003; Stich et al., 2006; Serpelloni et al., 2007), the geomorphological and geophysical data show evidences of recent ruptures and faults large enough to generate great earthquakes (Gràcia et al., 2006; Mauffret et al., 2007; Ballesteros et al., 2008; Maestro-González et al., 2008).

This area has suffered in the past several tsunamis, the main part of them with little impact, although damages to harbors and coastal inundations have been described (Soloviev et al., 2000; IGN, 2009b). The margins of the Alboran Sea are very developed areas, with increasing population and key to the tourism sector of the western Mediterranean, whether consolidated, such as the Spanish coast or emerging such as the North African. The recent experience of the 2003 Boumerdes–Zemmouri earthquake and tsunami has shown that even moderate events can produce sea waves with enough energy to cause significant economic losses. Tsunamis in the Alboran coast are historically more frequent than in the Balearic (IGN, 2009b), and given that the population and industrial development are higher in this area, an evaluation of the tsunami hazard seems necessary.

Even so, in the Balearic coast there are evidences of historical tsunamis, boulders above the sea level that only big waves could put there. Four zones have been studied in order to prove or localize boulders, often imbricated and above the sea level.

For the field work the boulders of four coastal zones have been studied, figure, 34.

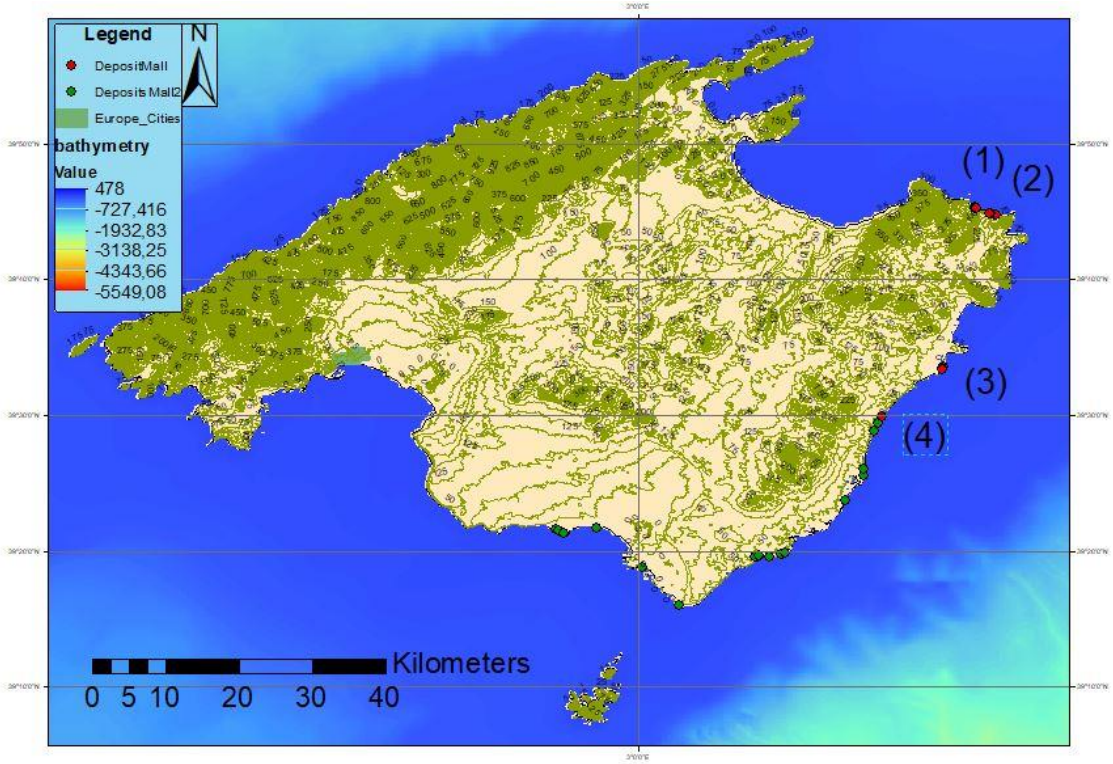

Figure 34: Field zones. (1) Cala Mitjana. (2) Cala Mesquida. (3) Cala Morlanda. (4) Cala Varques.

5.1 Cala Estreta and Cala Mesquida

Cala Estreta and Cala Mesquida are located at the North-East of the Mallorca Island as it can be seen in the figure 35. In these beaches there are a few boulders near the water, at a height of 3-5 meters above the sea level. In the figure 3.4 there are four boulders imbricated, the top boulder has a weigh of 8t approximately. Also in the figure 36, made in Cala Mesquida there are imbricated boulders.

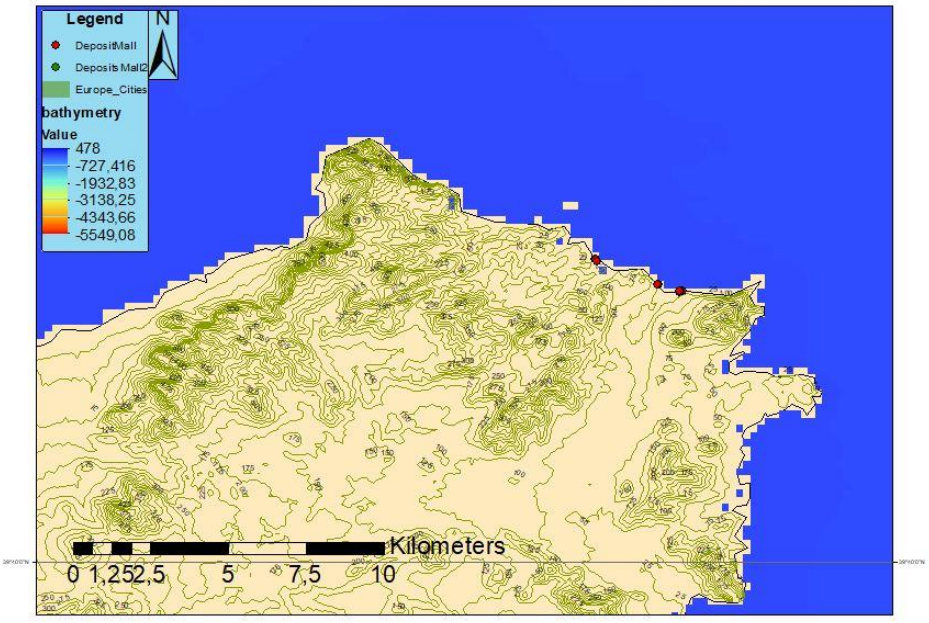

Figure 305: Localitzation of the Cala Estreta and Cala Mitjana zones, from the left to the right.

Figure 31: Imbricated boulders in Cala Mesquida.

5.3 Cala Morlanda and Cala Varques

Cala Morlanda and Cala Varques are located at the South-East of the Mallorca Island as it can be seen in the figure 37. In these beaches there are more boulders than in the other two sites and are higher above the sea level than Cala Estreta and Cala Mesquida, at a height of 8 - 10 meters above the sea level. In the figure 38 there are four boulders imbricated, the top boulder has a weigh of 12t approximately. Also in the figure 39, made in Cala Varques there are imbricated boulders.

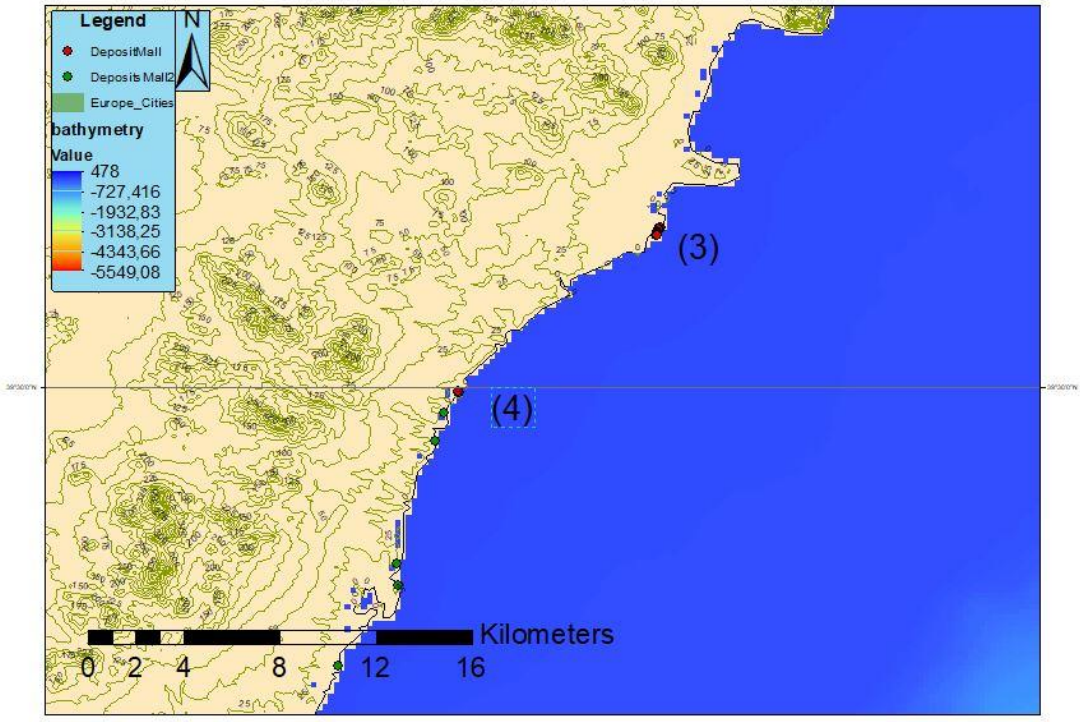

Figure 32: Cala Morlanda (3) and Cala Varques (4) ubication and orientation.

Figure 338: Boulder in Cala Morlando at the height of 8 meters above the sea level.

Figure 349: Cala Varques imbricated boulders.

5. Conclusions

In the last century or so, strong tsunamis and their causative processes were documented in the Mediterranean Sea and its connected seas from tide-gauge and other instrumental records, eyewitnesses accounts and pictorical material. The investigation of tsunamis in the historical and pre-historical periods is supported by a variety of documentary sources, onshore and offshore geological signatures including geomorphological imprints, and in some instances by field observations in selected coastal archaeological sites. Some of the Mediterranean region tsunamis were basin-wide, destructive events of large size produced either from earthquakes or from volcanic processes or even by aseismic landslides. One common feature that tsunami sources in the Mediterranean Sea share is that they are situated in the near-field domain, that is the travel times of first tsunami wave arrivals do not exceed half an hour or so. This feature is extremely critical from the point of view of tsunami risk mitigation, which is a lesson learned from several near-field, catastrophic tsunamis that occurred in the Pacific and Indian Oceans in the last 10 years or so (i.e. Sumatra 2004, Chile 2010 and Tohoku-Japan 2011). A global statistics has shown that 84% of the fatalities occurred within the first hour of tsunami propagation, and only 12% in the second (Gusiakov, 2009). This was corroborated by the large tsunamis of Chile 2010 and Tohoku- Japan 2011.

In this thesis the boulders repositioned by tsunamis, analysis and expansion via GIS software has been carried out. The potential hazard sources in the study area have been identified, those with a M_w7 or major earthquakes associated, and local phenomena as the 2003 minor tsunami in the Balearic harbours.

As the ASTARTE project summarize, the area between Colònia de Sant Jordi and the Cap de ses Salines, is exposed to earthquakes-generated tsunami from the North African margin, particularly from Algeria. In fact, along the coastal strip between Colònia de Sant Jordi and Cap de Ses Salines, extensive ridges made of large imbricate blocks up to ~24 tones in Wight and 5x3x1 m in size are viewed by some as evidences of paleo-tsunami deposits. Investigating such shallow environments in search of tsunami impact evidence is a challenge by itself, as this is a fringe impacted by regular high energy marine processes (i.e. storms) that tend to remove any sedimentary evidence of tsunamis except eventually for very large boulders and parent erosional surfaces. In contrast, deposits left inland by tsunami run-out at varying distances from the shoreline are relatively common and are widely used by paleo-tsunami research. It should also be mentioned that the tsunami resulting from the 2003 Boumerdes earthquake in Algeria hit the Baleares in the Late evening of the 21st of May sinking 200 boats despite the maximum run-up was slightly over of 1 meter.

Numerous coastal sites with meter-sized, several tons in weight, occasionally imbricated boulder fields occurring from almost present sea level to more than 20 meters in height beyond detachment surfaces atop of vertical sea cliffs occurs in the Balearic Islands. Given the wave regime, including storms, in the south-facing sites of occurrence of such boulder fields (i.e. oriented towards the North African margin, where the tsunamis hitting the archipelago are sourced) their most probable origin are tsunami waves with

anomalously high run-ups after they had been pushed against the sea cliffs. The detection of boulders fields like those found inshore below the present sea level has been attempted for the first time in the innermost continental shelf of Colònia de Sant Jordi, one of the test sites of the ASTARTE project. Many potential large boulders were found from present sea level down to 30 m depth. The boulders were not randomly distributed but mostly concentrated along contour parallel belts at 17-19 m, 34-38m and 41-44 m. Such depths ranges where boulders concentrate correspond to successive locations of a landward migrating coastline following the postglacial global sea level rise and are, therefore, indicative of the occurrence of tsunami impacts along the shores of the Balearic Islands and in the Western Mediterranean Basin further back in time than previously known

To realize the GIS map, the ArcGis software have been used for his simplicity of using layers. Every layer has the GCS_WGS_1984 Spatial Reference and the D_WGS_1984 Datum.

In the field zones of Cala Mitjana and Cala Mesquida, both on the north east of Mallorca, imbricated boulder that Roig-Munar et al., (2016) has identified like a non-tsunamigenic origin by his Transport Figure score, could be possible positioned by a tsunami wave diffraction as an effect of the low depth as it can be seen in the figure 4.9. In addition, the weight of some boulders measured with de Roig-Munar et al., (2016) equation weights more than 8 tones.

In the field zones of Cala Morlanda and Cala Varques the boulders are on a higher altitude than the first two zones and are bigger. This and the orientation toward the seismic zone, are the best indicators for the tsunamigenic origin of the boulders.

Further studies on the Balearic coasts should be realized. More accurate Transport Figures with a better porosity index could accurate the results of the Transport Figure equation. Also, the particular density of the blocs in each zone.

References

Álvarez-Gómez, José A., et al. “Scenarios for Earthquake-Generated Tsunamis on a Complex Tectonic Area of Diffuse Deformation and Low Velocity: The Alboran Sea, Western Mediterranean.” Marine Geology, vol. 284, no. 1–4, Elsevier B.V., 2011, pp. 55–73, doi:10.1016/j.margeo.2011.03.008.

Bahk, Jang Jun, et al. “Sedimentary Characteristics and Processes of Submarine Mass-Transport Deposits in the Ulleung Basin and Their Relations to Seismic and Sediment Physical Properties.” Marine Geology, vol. 393, Elsevier B.V, 2017, pp. 124–40, doi:10.1016/j.margeo.2017.05.010.

Behrmann, Sebastian Krastel Jan-hinrich, et al. Submarine Mass Movements and Their Consequences. Vol. 19, 2003, doi:10.1007/978-94-010-0093-2.

Baptista, Maria Ana. *Assessment, STrategy And Risk Reduction for Tsunamis in Europe*. no. 603839, 2015.

Casciello, Emilio, et al. “The Alboran Domain in the Western Mediterranean Evolution: The Birth of a Concept.” Bulletin de La Société Géologique de France, vol. 186, no. 4–5, 2015, pp. 371–84, doi:10.2113/gssgfbull.186.4-5.371.

Coderque, Jose Turmo. Projecte O Tesina D ’ Especialitat. 2011, pp. 1–59.

Lüdmann, T., et al. “Southwest Mallorca Island: A Cool-Water Carbonate Margin Dominated by Drift Deposition Associated with Giant Mass Wasting.” Marine Geology, vol. 307–310, Elsevier B.V., 2012, pp. 73–87, doi:10.1016/j.margeo.2011.09.008.

Maouche, Said, et al. “Large Boulder Accumulation on the Algerian Coast Evidence Tsunami Events in the Western Mediterranean.” Marine Geology, vol. 262, no. 1–4, Elsevier B.V., 2009, pp. 96–104, doi:10.1016/j.margeo.2009.03.013.

Maramai, Alessandra, et al. “The Euro-Mediterranean Tsunami Catalogue.” Annals of Geophysics, vol. 57, no. 4, 2014, doi:10.4401/ag-6437.

Marcos, Marta, et al. “External Forcing of Meteorological Tsunamis at the Coast of the Balearic Islands.” Physics and Chemistry of the Earth, vol. 34, no. 17–18, Elsevier Ltd, 2009, pp. 938–47, doi:10.1016/j.pce.2009.10.001.

Masina, M., et al. “Tsunami Taxonomy and Detection from Recent Mediterranean Tide Gauge Data.” Coastal Engineering, vol. 127, Elsevier Ltd, 2017, pp. 145–69, doi:10.1016/j.coastaleng.2017.06.007.

Papadopoulos, Gerassimos A., et al. “Historical and Pre-Historical Tsunamis in the Mediterranean and Its Connected Seas: Geological Signatures, Generation Mechanisms and Coastal Impacts.” Marine Geology, vol. 354, Elsevier B.V., 2014, pp. 81–109, doi:10.1016/j.margeo.2014.04.014.

Papadopoulos, Gerassimos, and Gerassimos Papadopoulos. “Chapter 2 – Historical and Geological Evidence of Tsunamis in Europe and the Mediterranean.” Tsunamis in the European-Mediterranean Region, no. 1960, Elsevier Inc., 2016, doi:10.1016/B978-0-12-420224-5.00002-8.

Roger, J., and H. Hébert. “The 1856 Djijelli (Algeria) Earthquake and Tsunami: Source Parameters and Implications for Tsunami Hazard in the Balearic Islands.” Natural Hazards and Earth System Science, vol. 8, no. 4, 2008, pp. 721–31, doi:10.5194/nhess-8-721-2008.

Roig-Munar, F. X., et al. “Indicadores Geomorfológicos de Tsunamis Históricos En Las Costas Rocosas de Baleares.” Geo-Temas, vol. 16, no. 1, 2016, pp. 641–44.

Schedule, Estimated, et al. MALLORCA FIELD TRIP.

Scheffers, A. “Tsunami Boulder Deposits.” Tsunamiites - Features and Implications, Elsevier B.V., 2008, doi:10.1016/B978-0-444-51552-0.00017-5.

Sorensen, R. M. “Basic Coastal Engineering Basic Coastal.” *Environmental Engineering*, 2006, doi:10.1007/b101261.

Vela, J., Pérez, B., González, M., Otero, L., Olabarrieta, M., Canals, M., Casamor, J.L., 2014. Tsunami resonance in Palma bay and harbour, Majorca Island, as induced by the 2003 Western Mediterranean earthquake; The Journal of Geology, 122: 165-182. Doi: 10.1086/675256.

Websites

EMODnet portal (http://portal.emodnet-bathymetry.eu/)

Margin Regions (http://www.marineregions.org/downloads.php#iho)

ATARTE desposits points (https://www.arcgis.com/home/webmap/viewer.html?webmap=4eea1187ed1b4ccd889e533b1667e4ab&extent=-72.2569,1.5325,101.3271,72.7755)

Euro-Mediterranean Tsunami Catalogue (http://www.arcgis.com/apps/StorytellingTextLegend/index.html?appid=8329c2ad9b7f43c18562bdddc6c1ad26)

USGS (https://earthquake.usgs.gov/data/comcat/)

ISC (http://www.isc.ac.uk/iscgem/download.php)

Open DEM (http://www.opendem.info/opendem_client.html)

Efraín Porto Tapiquén (https://tapiquen-sig.jimdo.com/english-version/free-downloads/europe/)

Tsunami: Basic Principles (https://pdhonline.com/courses/g207/g207content.pdf)